LA-6402-P

Proposal

Special Distribution

Reporting Date: June 1976
Issued: July 1976

A Proposed 10-MJ Fast Discharging Homopolar Machine for Fusion Reactor Systems

by

J. D. Rogers
K. I. Thomassen
C. J. Mole*

*Westinghouse Electric Corp., Research and Development Center, Beulah Road, Pittsburgh, PA 15235.

los alamos
scientific laboratory
of the University of California
LOS ALAMOS, NEW MEXICO 87545

UNITED STATES
ENERGY RESEARCH AND DEVELOPMENT ADMINISTRATION
CONTRACT W-7405-ENG. 36

Work supported by Electric Power Research Institute.

CONTENTS

A PROPOSED 10-MJ FAST DISCHARGING HOMOPOLAR MACHINE FOR FUSION REACTOR SYSTEMS

by

J. D. Rogers, K. I. Thomassen

Los Alamos Scientific Laboratory
P. O. Box 1663
Los Alamos, New Mexico 87545

and

C. J. Mole

Westinghouse Electric Corp.
Research & Development Center
Beulah Road
Pittsburgh, PA 15235

ABSTRACT

A developmental program is proposed to complete the design and to fabricate a 10-MJ, 30-ms discharge homopolar machine. The work will include component development and testing of critical subassemblies which advance the state-of-the-art. The final homopolar machine will be tested in circuits to determine its performance as a potential fusion energy storage source.

I. SUMMARY

During the past several years the technical and economic requirements for very fast energy delivery systems from a few up to hundreds of milliseconds for fusion reactors have been emerging. The most notable examples involve high-β fusion systems in which capacitive storage, now in use, is not feasible for larger future generation devices. This has prompted intensive investigations of alternative energy storage systems and identified the need to advance the technology.

The transition from capacitive storage to some alternative storage system was first specified in the Scyllac Fusion Test Reactor[1] (SFTR) by requiring a superconducting Magnetic Energy Transfer and Storage[2] (METS) system. In the Reference Theta Pinch Reactor[3] (RTPR), a METS system is required for staging between the implosion and compression fields.

Inertial storage has also been proposed for fusion systems, the earliest proprosal being the NRL imploding liner system[4] with a self-excited, homopolar machine. More recently, the RTPR design has incorporated modules of homopolar machines to provide compressional field energy to bring the plasma to ignition. The energy is subsequently recovered at high efficiency, a necessary feature to achieve an energy balance in the reactor. Westinghouse, in a design study[5] for the Los Alamos Scientific Laboratory (LASL), first identified the potential economic advantage of homopolar machines for the RTPR. A subsequent study[6] gave more detail to the machine and considered other system problems.

Over the past year, Westinghouse (W), the University of Texas (UT), and LASL have participated in a further design study, sponsored by the Electric Power Research Institute (EPRI), of the RTPR homopolar. The first phase of that study led to a fairly extensive conceptual engineering design[7] of the machine, which was used to determine the scale size model machine to construct for testing key features of the machine. That model, a 10-MJ, two-rotor machine, is now in final engineering design under the EPRI study. The construction of that machine and its initial testing at W and LASL are being proposed here. Funding by EPRI and ERDA is requested, totaling $3.2 M over a three-year period, commencing in FY77. This is a joint proposal from Westinghouse and LASL.

We view the model machine as a test of several new technologies and their systems integration, which are fundamental to homopolar machines for a variety of fusion devices. We have identified a potential role for homopolar machines in tokamaks, high-β systems, and lasers and have described these in this proposal. The machines differ in the amount of energy they store, their energy delivery times, and their internal impedance. However, gigajoule sizes, tens to hundreds of millisecond delivery times, and high voltages are quite typical.

The problems addressed by the model machine relate to these requirements and in particular to the high-surface speeds, high-current density collection system, and high magnetic fields which are necessary to achieve the requirements. The speed and high field are required for high voltage and the high current to extract large energies in short times. These features lead to brush and current collection problems, questions of stress and stability in the rotors, cooling problems, and problems associated with large superconducting magnets. The model machine cannot address all the specific questions of machines designed for all the fusion systems, but it will make necessary and significant advances in the state of the art for machines of this general nature. The RTPR machine is well posed and is of greatest interest to LASL; hence, we have chosen to direct our efforts on the model machine specifically for the RTPR requirements.

This proposal describes the role of homopolar machines in high-β systems (Section II) and in other fusion applications (Section III). The design studies for RTPR are summarized in Section IV, and our program plan under this proposal is described in Section V. Costs and schedules are given in Section VI, and ideas for using the 10-MJ machine for LASL physics experiments and for further machine development are presented in Section VII. Section VIII deals with the proposed administration of the work.

II. HOMOPOLAR MACHINES FOR HIGH-β SYSTEMS

Designs for several high-β reactor devices have proceeded to the point where the requirements on pulsed energy supplies can be set and the role of a homopolar machine assessed. In the case of the RTPR, machine parameters have been specified for concreteness in the program of machine development.

The RTPR uses fifty machines, 1.3 GJ each, which deliver energy in 30 ms. Section IV describes the design in greater detail, but the unique features are a superconducting field coil, rotor surface speed of 277 m/s, and 11-kV output from eight rotors. The circuit in Fig. 1 illustrates the application, and the waveform shows the RTPR power cycle.[3,5] The compression time T_c and quench time T_q are 30 ms, and the burn time T_b is 70 ms. The total cycle time T_t is either 3 or 10 s, depending on the acceptable plasma wall loading.

In a circuit analysis the homopolar machine is analogous to a capacitor and will resonate with an inductor. Since almost all fusion applications involve delivery or removal of energy from an inductor, this high efficiency circuit finds universal application. Further, the machine can efficiently store energy between pulses, also an important feature.

Another application has been defined in linear theta pinch systems. A hybrid fusion-fission reactor has been designed[8] at LASL, and the only high-efficiency power conversion scheme presently identified to drive that device is a homopolar. Designs call for units which pulse 1-4 times a second, with 1- to 4-ms pulses (half-sine waves). This delivery time is at the limit of what is felt technically feasible if efficiency is to be kept high. Specific machine designs have been advanced[9] for use in a circuit like that shown in Fig. 2. Approximately 200 machines, rated at 125 MJ each, are required for a 1-km-long hybrid reactor. No crowbar switch (S_2) is required to synthesize the half-sine waveform, and switch S_1 opens and closes at a current zero.

Imploding liner reactor designs have been pursued at NRL and at the Efremov Institute in Leningrad. These designs are somewhat more preliminary than the theta-pinch designs but are sufficient to indicate the range of energies and discharge times required. Roughly, 10 GJ must be delivered in 0.1-1.0 ms at high voltage (high impedance) to a variable inductance. Both the NRL and Efremov designs consider homopolar machines for this application.

III. HOMOPOLAR MACHINES FOR PULSED ENERGY APPLICATIONS

Both tokamaks and toroidal z-pinches plan to use ohmic heating to bring the plasma to, or near, ignition. This requires the transfer of several gigajoules of energy in $\sim$ 1 s between the ohmic coils and intermediate storage. The homopolar resonant transfer may be well suited to this task.

The machines for ohmic heating share many of the same technical problems as those for shorter transfer times, namely those associated with high-voltage,

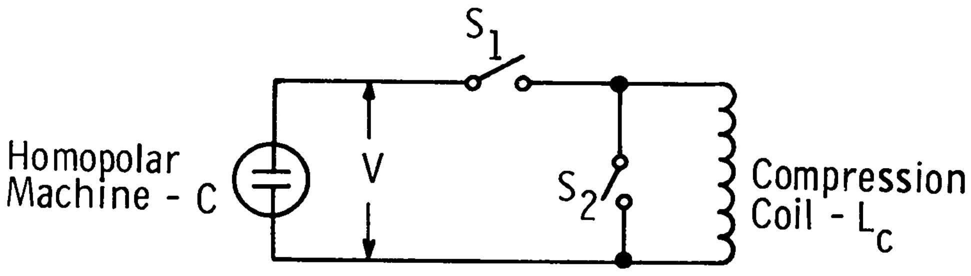

LC Circuit

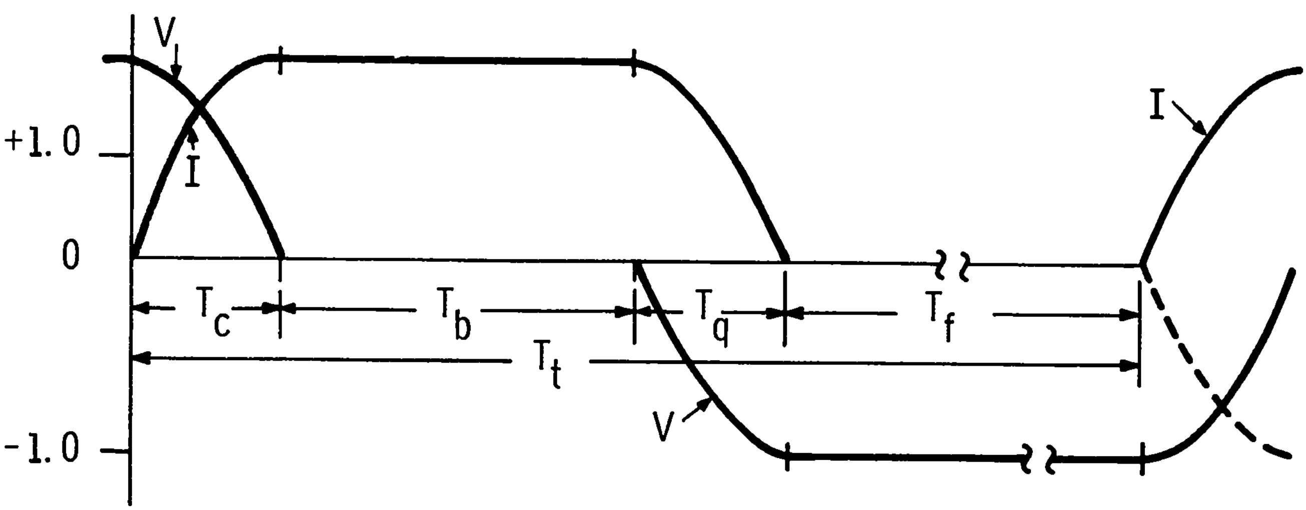

Voltage and Current vs Time

Fig. 1. Homopolar Energy Transfer and Storage System (HETS).

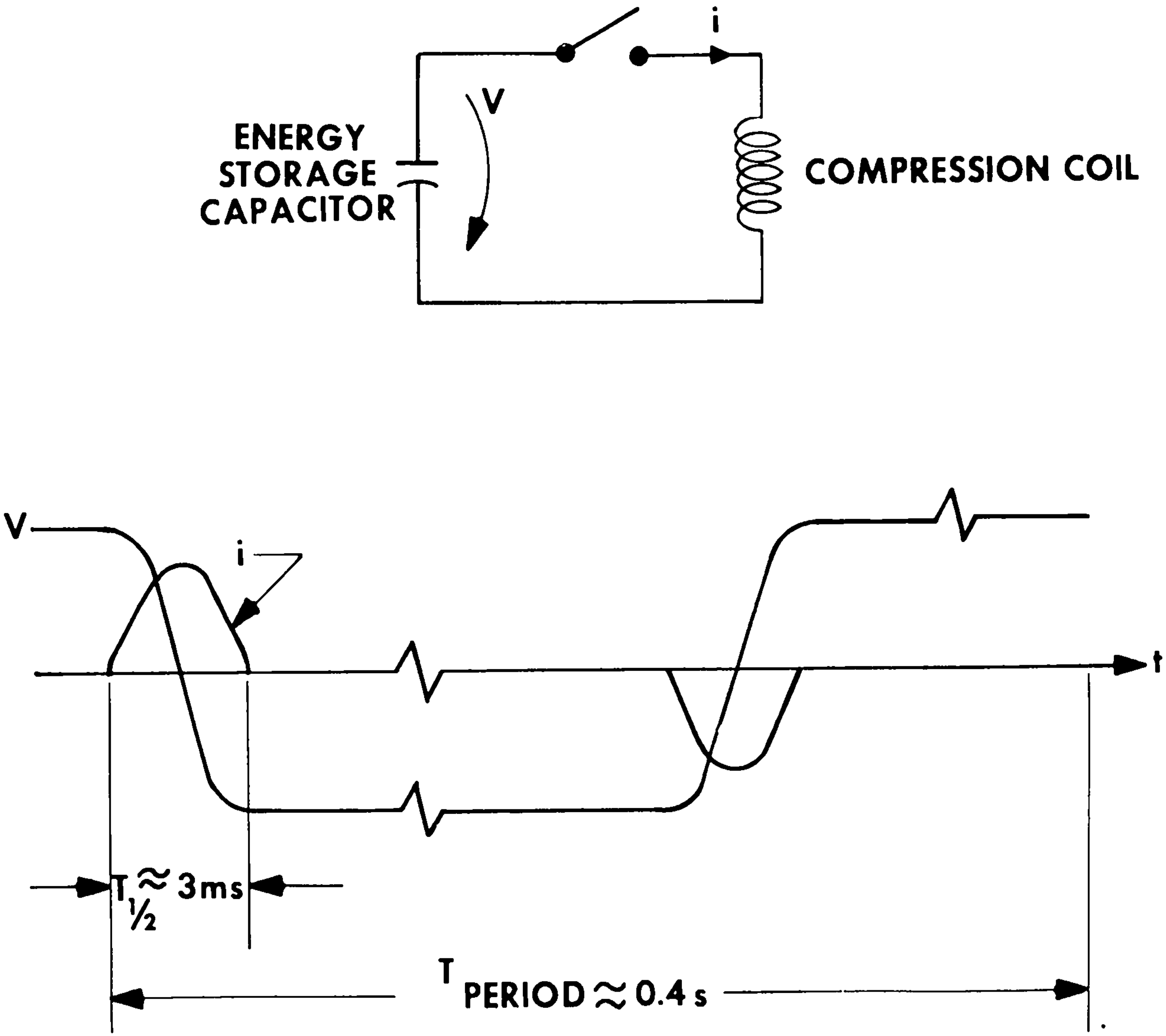

Fig. 2. Hybrid Fusion/Fission Reactor Compression Coil Circuit.

high-current, high-field, and high-surface speeds. In addition, the longer discharging times lead to higher brush thermal loading, but stresses associated with rapid deceleration are smaller.

Design studies at UT, W, and LASL on the ohmic-heating system requirements, cost analyses of alternative systems, and specifications of developmental programs leading to Experimental Power Reactor (EPR) scale systems are under way. Any homopolar development specifically for ohmic-heating systems will benefit substantially from information developed by the proposed 10-MJ model.

Another general area of interest is the rapid charging of room temperature storage coils by a homopolar. The storage coils' energy is subsequently transferred more rapidly to a load by interrupting the storage coil current. A homopolar machine may be applied in this manner when the transfer time is too rapid for direct homopolar delivery. The use of intermediate inductive storage for 30- to 300-μs energy transfer times is indicated for large laser flash lamp supplies, for liners if times shorter than the 1 ms quoted earlier become necessary, or for the METS system in SFTR or RTPR.

For the SFTR parameters the homopolar was found to be the least expensive charging system when both the charging supply and storage coil costs are considered. Fast charging, in times less than the coil L/R time, allow smaller conductors (less copper) and, therefore, lower cost coils. An optimum transfer time for minimum system cost exists since homopolar costs (per joule) increase with shorter discharge times. For SFTR, an optimized system for transferring ∿ 500 MJ was designed by W, resulting in a 300-ms discharge machine.[10]

IV. DESIGN STUDIES FOR HIGH-β SYSTEMS

A. RTPR Machine Design

The large amounts of circulating energy in fusion reactors indicate that the efficient transfer and recovery of magnetic energy from both pulsed theta-pinch fusion reactors and tokamak ohmic-heating systems is a stringent but necessary requirement for a favorable energy balance. Early reactor designs established the size of the energy store, typical delivery times, efficiencies, and cost constraints. A search for possible technical solutions to the problem has led to the consideration of a variety of systems, including superconducting storage and switching by mechanically changing mutual circuit inductances,[11] short circuit generators, motor-generator sets with rectifier-inverter systems, superconducting storage with resonant transfer using homopolar machines as "capacitive" transfer elements, and finally superconducting homopolar machines with direct transfer initiated vacuum arc switches.

Studies[5] were conducted to determine which of these systems were the most promising for theta-pinch systems. It was very clear that only superconducting storage with variable inductance switching and direct coupled homopolar machines could conceptually meet the requirements. Of these, the homopolar machine is much closer in concept to present-day electromechanical devices and was also the lowest cost system. Consequently, a more detailed system analysis of the RTPR application, including consideration of the load, optimum module size for minimum cost, switching techniques, etc., was undertaken by Westinghouse under AEC contract. A sharper definition of the machine design and some preliminary detail of its construction emerged from that study.[6]

The energy storage and transfer system for the RTPR[3] must deliver 63 GJ with a 30-ms rise time, 70-ms hold, and 30-ms fall. The energy must be cycled with approximately 95% efficiency. The system design uses 50 machines and numerous interrupting switches, costing approximately 0.9¢ per joule. Each 1.3-GJ machine delivers 12.25 MA at 11 kV and consists of eight drum-type rotors, alternately rotating in opposite directions. While a more recent Westinghouse report[6] defined the central design concepts, detailed analysis of the thermal, mechanical, and electrical systems and design interactions based on these analyses are the subject of a contract with EPRI. The results to date of that effort are covered in monthly progress reports and the 1975 semiannual report.[7]

The RTPR homopolar machine, shown in Fig. 3, has approximately 13 m of active rotor length, with approximately 2-m diameter rotors that spin at 277-m/s peripheral speed in a hydrogen atmosphere. The magnetic field is based on the development of Nb_3Sn magnets to operate with a peak field of approximately 80 kG at the conductor. The rotors are supported by conventional oil bearings on a central shaft. Flux return is provided by an iron yoke outside the superconducting coils, while current returns through a hollow cylindrical conductor between rotor and coil. The copper graphite brushes are mounted inside the rotor with eleven rows of brushes on each end of each rotor.

The rotor is to be constructed from graphite fiber reinforced aluminum to have the required fatigue life. The design here is presented in terms of the required material properties, both electrical and mechanical, and an assessment of

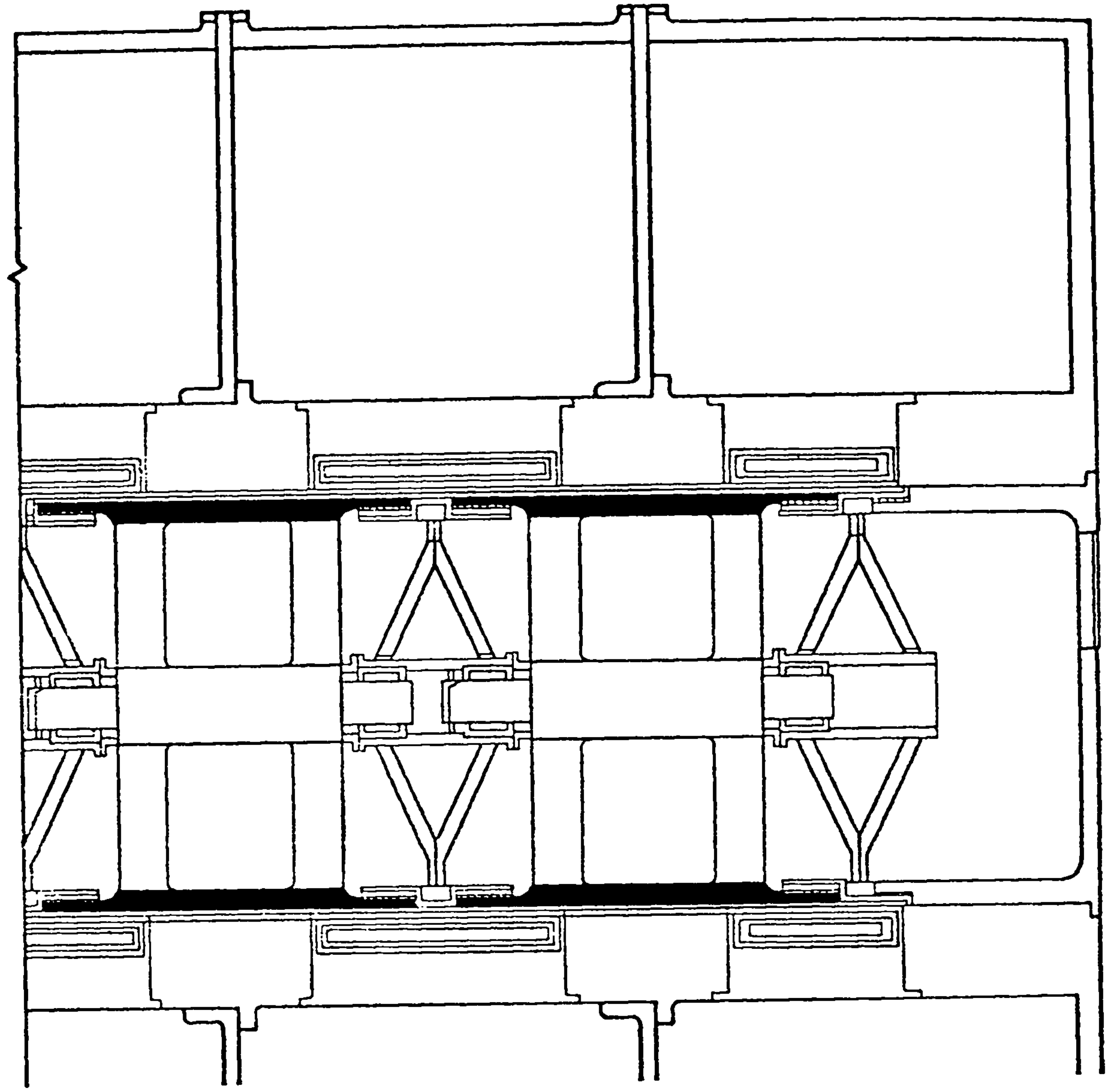

CAPACITY	1290 MJ	COLLECTOR LENGTH	0.25 m
No. ROTOR MODULES	8	STATOR OD	3.2 m
ROTOR DIAMETER	2.17 m	FLUX SHIELD OD	7.0 m
ROTOR PERIPHERAL VELOCITY	277 m/s	OVERALL LENGTH	20 m

Fig. 3. The Two End Rotors and Structure of a 1.3-GJ Homopolar Machine.

the state of the art as it relates to producing these materials in the future. The fabrication of such materials is at an early stage of development but there is promise that the industry will mature soon. An all aluminum rotor could be used with a reduced fatigue life for early construction of the machine.

The efficiency of the machine has been calculated, and the losses in switching and transmission were estimated. The overall system efficiency - energy returned to rotor inertia compared to initial stored energy - is 95.2%. The machine losses alone are approximately 3.6%. The cost of the machine is $6.55 M, or 0.51¢/joule, based on constructing three RTPR plants a year in a developed fusion economy. These values of cost and efficiency are quite attractive and make the RTPR energy transfer scheme a viable one.

To demonstrate the practicality of such a machine the present EPRI contract calls for the detailed engineering design of a scaled-down model of the 1.3-GJ, RTPR machine. The first phase of the contract, however, required an extensive conceptual design of the full scale machine in sufficient detail to identify technical problem areas which need be addressed by a scaled version. In this way the rationale for the scaled machine has a firm technical base.

The design of the 1.3-GJ machine has been completed by Westinghouse and the University of Texas with LASL guidance. There have been several iterations of the design and some early decisions on various concepts. A disc-type machine for fast discharging had been examined prior to this contractual period by the University of Texas,[12] and their initial design leaned that way. However, it was soon recognized that this configuration was advantageous for extremely fast discharges ($\sim$ 1 ms) but suffered by comparison with the drum machine proposed by Westinghouse when efficiency was the primary concern.

The machine is modularly constructed and is composed of rotor modules, current collectors, an iron stator, stator conductor, and excitation coils, as shown in Fig. 4.

The machine is constructed by segmenting the stator and the magnetic circuit in a manner such that each intermediate excitation winding produces a magnetic field for adjacent modules.

A relatively unique feature of the machine is the rotating element. The rotor in each module consists of a radially thin hollow aluminum cylinder. This rotor design permits a low ratio of stored kinetic energy to electrical power rating (watt-seconds/watt) while maintaining high electrical utilization of the mass of material.

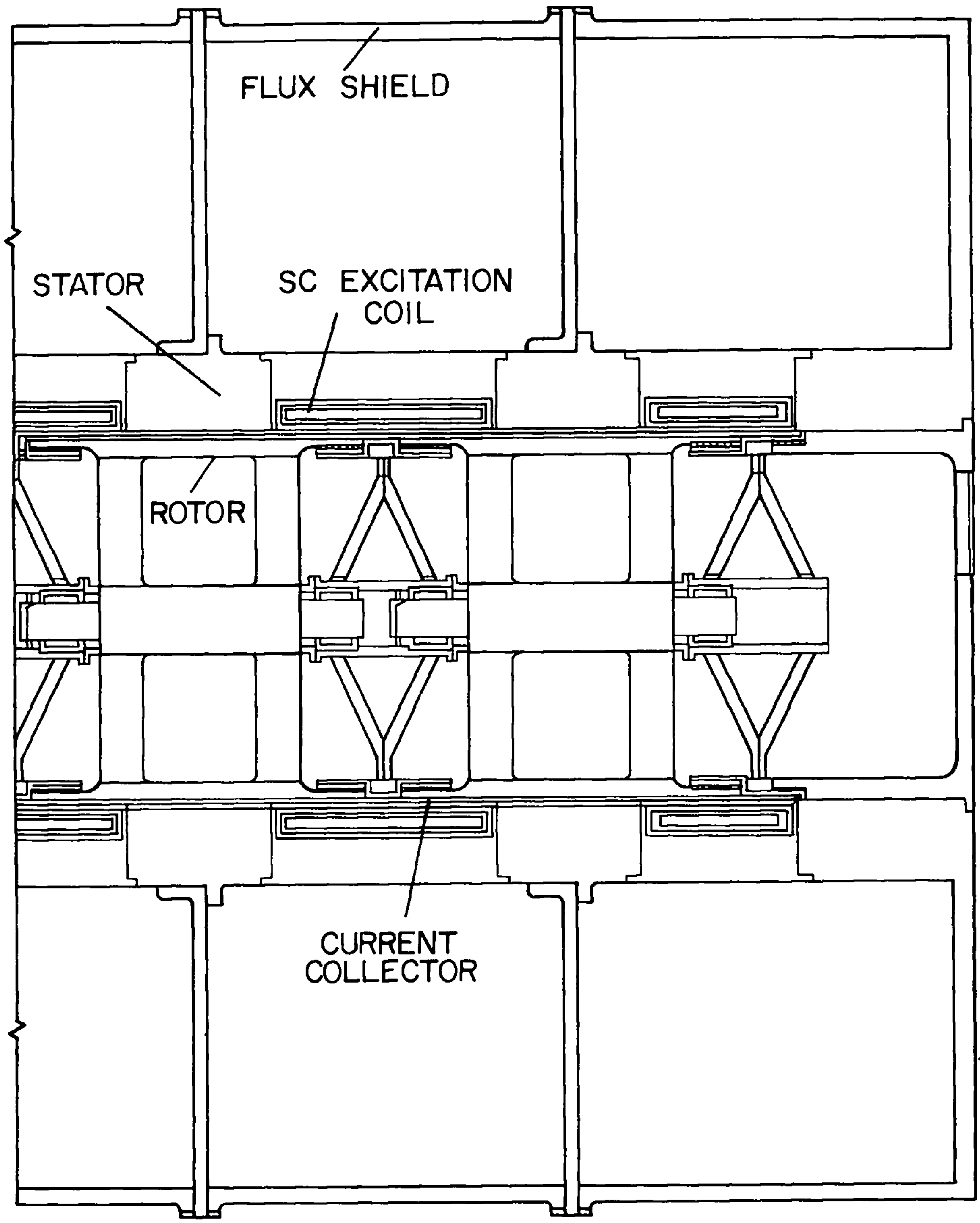

Fig. 4. Homopolar Machine General Arrangement.

Current is collected at each end of the rotor through integral slipring and metal-graphite brushes. The aluminum rotor brush tracks require cladding with a more suitable material for current collection such as copper.

The iron stator surrounding the rotor serves as a magnetic flux path which passes the flux radially through the rotating cylinder. Since the flux is directed in one radial direction with respect to the rotor, the configuration fits the definition of a homopolar machine.

Excitation coils located at each end of the module produce the magnetic field. Superconducting excitation windings are employed to develop the large magnetomotive force and a resulting average field intensity of 30 kG passing through the rotating conductor. The high level of performance predicted for the machine in terms of electrical output and efficiency are results of the relatively high field intensity which can be achieved through superconductivity.

A stator conductor which is stationary provides the return circuit for the current. The return circuit takes the form of a thin wall copper cylinder which is insulated and supported in the bore of the stator. This configuration, in which the rotor cylinder rotates within the return circuit cylinder with currents in oposite directions, is effective in minimizing the machine inductance and the related magnetic energy loss during the energy transfer cycle. The machine is closed and sealed and contains hydrogen to minimize windage losses.

The machine has been optimized from considerations of costs and energy losses. The RTPR studies included analysis for the energy transfer losses to minimize plant cost per unit of energy produced.

In addition to the cost and loss considerations, there are fundamental limitations imposed on the number, size, and energy level of the modules used in constructing the machine. These are functions of magnetic configurations, mechanical stress, etc.

These considerations lead to the following parameters which were fixed for all configurations investigated.

Rotor Peripheral Velocity	277 m/s
Radial Magnetic Field (Ave.)	30 kG
Rotor Active Length-to-Diameter Ratio	3/4

At these speed and field conditions, the voltage developed is 831 V per meter of active rotor length. To develop 10 800 V per machine (required for each of two machines in series to match the compression coil), the total active length required is about 13 meters. This fact coupled with the length-to-diameter ratio forms a basis for candidate module sizes. Practical considerations of the size and weight in terms of handling, transportation, and erection favored the eight rotor machine. Within these bounds, energy density and rotor diameter were optimized. The studies led to the selection of the eight-rotor machine.

The principal electrical and physical characteristics for the homopolar machine selected for design are listed in Table I.

From the optimization analysis a list of the principal components and their cost were developed and are given in Table II. The total cost of the 1290-MJ machine is 6.55 million dollars.

The energy losses associated with the machine are based on one complete cycle which is repeated at ten-second intervals. The losses are tabulated below for each category. The total loss for the machine is 3.57% of the energy stored. The loss estimate for the system which includes the support systems is 4.8%. These are given in Table III.

A more extensive tabulation of the homopolar machine characteristics is presented in Table IV.

A number of design considerations have been examined in great detail. These include the electrical design, mechanical and thermal analysis, stress analysis, rotor dynamics studies, the superconducting field coil, and design of the current collection system.

The electrical design included the fundamental voltage, current, and impedance relationships. Extensive finite element computer programs were used to

TABLE I

PRINCIPAL HOMOPOLAR CHARACTERISTICS

Capacity	1290 MJ
Voltage (max)	11 kV
Current (max)	12.25 MA
Discharge Time	30 ms
No. Rotor Modules	8
Rotor Diameter	2.17 m
Collector Length	25 cm
Brush Current Density	1550 A/cm^2
Brush Packing Factor	0.5

TABLE II

HETS-MACHINE COST

Finished Component	Estimated Cost M$	Estimated Cost %
Iron-Stator & Shield \$.81/lb	1.58	24
SC Magnet \$28.90/lb	1.68	26
Stator Conductor \$4.13/lb	.33	5
Rotor \$9.50/lb	.95	15
Current Collection System \$31/in^2	.61	9
Brg., Struct., Assy., Test	1.40	21
Machine Complete	6.55	100
Specific Cost	5.08 mills/joule	

TABLE III

1.3-GJ HOMOPOLAR LOSSES

Loss Category	Loss - %
Rotor Drum - I^2R	1.06
Rotor Interconn - I^2R	0.17
Stator Cond. - I^2R	0.78
Magnetic	0.79
Collectors	
Electrical	0.27
Mechanical	0.21
Windage	0.24
Bearing	0.05
Total Machine	3.57
Transmission	0.10
Switch	0.97
Refrigerator	0.20
Total System	4.84

TABLE IV

REFERENCE DESIGN CHARACTERISTICS
SINGLE COIL - THIN SHIELD

Rotors - 8
Capacity - 1290 MJ
Voltage - 11,100 V
Current - 12.25 x 10^6 A
Discharge Time - 0.03 s
Rotor Diameter - 2.167 m (85.3 in.)
Drum Length - 2.06 m (81 in.)
Outer Shield Dia. - 7.06 m (278 in.)
Length - 23 m (904 in.)
Shield Weight - 0.89 x 10^6 kg (2.0 x 10^6 lbs.)
Iron Shield Flux Density - 18 kG
Average Gap Density - 29 kG
Average Axial Density - 50 kG
Peak Field - 80 kG
Coil Current Density - 13,950 A/cm^2 (90,000 A/in^2)
Filling Factor - 0.592
Coil Stored Energy - 1025 MJ
Superconductor Weight - 25,800 kg (57,000 lbs.)
Collector Diameter - 2.083 m (82 in.)
Collector Length (Brush ℄ to ℄) - 25.4 cm (10 in.)
Average Radial Field - 15 kG
Average Axial Field - 55.4 kG
Average Collector Surface Angle - 15°

establish the magnetic field. An iterative design comparison on the basis of peak fields, field coil ampere - turns per module, iron shield weight, flux leakage, and magnetic field pattern at the brushes was performed to establish the final configuration.

The mechanical design provides for spoke-mounting of the drum to the shaft although disc mounting is worthy of further design effort to eliminate out-of-roundness problems. Hydrodynamic pivoted pad oil lubricated bearings support the shaft. The stator strut assembly fastens to a special structure and the magnetic shield. It is intended that the machine will be supported by foundation feet attached to the magnetic shield. The entire rotor support system is designed with sufficient stiffness to insure operation below the first critical speed in all three modes - whirl, axial, and torsional. The stator return conductor is a cylindrical copper shell with penetration only in the area of the stator strut assembly support foundations. The stator return conductor is insulated from the stator iron. The superconducting excitation coils are mounted in the stator iron using fiber glass composite support struts. The superconducting coil is wound into a segmented Inconel support structure. The low-temperature zone is surrounded by a radiation shield to reduce radiation losses. A preloaded double acting thrust bearing is provided to maintain the axial positioning of each rotor. The thrust and radial support bearings will be electrically insulated from the support structure to prevent ground leakage currents. The design of the rotor and the superconducting coil structure were identified early in the program as critical. The material selection for the rotor drum requires a metal that is both a good electrical conductor and has sufficient structural strength to withstand the forces developed from rotation, acceleration, and deceleration. The design of the superconducting coil structure must consider the forces developed due to the interaction of the coil current with the magnetic field. With respect to the coil cross section, these forces may be resolved into radial and axial components. The forces are functions of coil geometry, current, and the flux density distribution within the cross section of the coil. Besides the axial and radial loads, forces arising from coil misalignment were included in the mechanical design.

The thermal design was composed of analyses of the steady state surface temperature, transient rotor temperature, rotor windage, hydrogen flow losses, brush thermal analysis, steady state brush temperature, and transient brush surface temperature.

The stress analysis concentrated mostly on the superconducting coils and the rotor drum. The other structural integrity problems of the machine were routine and readily solved. The loadings which cause significant stresses in the rotor are mechanical, thermal, and electromagnetic. The most significant loading is the radial body force due to the steady spinning of the rotor at 256 rad/s. Not only is this the load of greatest magnitude, but it is cyclic in nature occurring at a frequency of approximately $3(10)^6$ cycles/year. This spin induced loading results primarily in a uniform hoop tension in the drum. Secondary effects which must be evaluated include bending in the axial plane due to differential growth, if any, between drum and spokes and between the thick drum and the thin current collecting ring. The thermal loading of the rotor has been assumed to be due to a spatially uniform temperature change of 100°F. The composite drum experiences far less growth due to temperature change than do the spokes and shaft which have a much higher coefficient of expansion. It is envisioned that the connection between spokes and drum will be affected at the elevated temperature (i.e., the assumed operating condition). The stresses and deformations due to thermal loading will, in such circumstances, occur upon the cooling of the rotor to room temperature. The stresses thus induced include tension in the spokes and in the composite at the point of spoke attachment, as well as bending stresses in the circumferential and axial directions. This loading is repeated only upon shutdown of the machine and so the resulting stresses do not contribute to fatigue of the material.

As the machine discharges, current flows axially along the drum, cutting the radial component of the magnetic field, the resulting I x B torque decelerates the rotor. Because the current diffusion time for the thick rotor is more than the discharge time, the current is effectively confined to a skin depth of 4.0 cm (1.57 in.). Thus the decelerating forces, acting over an outer layer of the drum, decelerate the rotor by means of shear stresses. These stresses act on surfaces of constant radius in the tangential direction. Although the current is uniform along the length of the rotor, the strength of the radial component of field is not. Thus, that portion of rotor in which the radial component is maximum tends to produce more than its share of decelerating torque. This torque is transmitted to the remainder of the rotor through shear stresses.

Studies of the rotor dynamics considered steady state vibrations and transient discharge effects. The first is associated with spinning such a large rotor at the proposed speeds, and the latter is due to a complex interaction between the applied field, the brushes, the return conductor, and the rotor. This problem is unique to this type of machine and has, therefore, had very little prior study. Several steady state vibrational modes of the rotor were investigated to insure that there would not be excessive vibrations of the machine at operating speed. Many of these modes such as the hoop ringing of the rotor and shaft bending which may have been significant during the evolution of the design are now clearly far removed from the operating speed of the final conceptual design. The more significant vibrational modes are those involving the rotor-bearing bearing support system and one internal rotor vibration that will be discussed below. Symmetrical and nonsymmetrical bearing support structure transverse vibrational modes were examined by finite element computational methods. Axial loading of the thrust bearings was considered. The entire bearing support system was analyzed as a spring-mass-damper system with three modes of rotor motion considered. The driving function was assumed to be sinusoidal. The three modes were a simple axial translation, a transverse translation, and a transverse rotation. The fourth steady state vibration investigated was for torsional oscillation of the outer portion of the rotor about the central shaft. This mode affects the stiffness of the spokes. The design is such that none of the vibrational modes are within the machine operating range.

Ideally, the dynamic discharge forces generated to stop the rotor are applied circumferentially to the rotor and return conductor and there are no forces or moments applied to the rotor in other directions. The peak torque required to stop the rotor is approximately 67×10^6 N-m. Clearly, even a small portion of this torque applied in another direction has the capability of causing serious problems. Misalignment of the rotor inertial or mechanical axis and the electrical axis and current and magnetic fields asymmetries can also create unusual forces, particularly during discharge. These types of conditions have been analyzed and require further consideration to complete the design.

The superconducting field coils require a conductor which can carry very high-current densities at high fields. Multifilament conductors, which are mandatory because of stability considerations, are commercially available today in NbTi, while Nb_3Sn conductors are still developmental. A NbTi conductor with a 2:1 copper to NbTi volume ratio, which is the lowest copper content to consider, has a critical current density of 25 kA/cm^2 at 85 kG, only 6% above the design operating point. The projected Nb_3Sn conductor has a corresponding current density as high as 60 kA/cm^2, more than double the proposed operating point. In addition, the higher critical temperature of Nb_3Sn makes it less sensitive to temperature fluctuations due to refrigeration transients or a.c. losses during the machine discharge or charge cycle. The conductor envisaged here contains approximately 55% Cu, 33% Cu-Sn bronze, and a 12% mixture of Nb_3Sn, Nb, and Ta. A monolithic conductor can possibly be used for these coils. Conductors of this type have been fabricated and tested in coils.[13,14] The overall conductor size is 1.09 x 0.39 cm bare and 1.14 x 0.44 cm insulated consistent with a 10-kA current. The coils in the machine are excited in opposition to one another and large axial forces are exerted on each coil. For the interior coils this force is 88.1 x 10^6 N and 35.6 x 10^6 N for the end coils. The coils are electrically in series and are designed for full axial support on the end coils and 3.6 x 10^6 N in either axial direction on the central coils to handle any unbalanced forces due to coil winding or placement errors. The coil temperature rise on quench is less than 100 K. The coils will be insulated for a discharge voltage level of 20 kV. The coils are wound within an Inconel shell which supports both radial and axial forces. The axial forces are taken up by radial webs of varying thickness so that each coil is, in effect, several coils in series. The cryogenic system will be designed such that helium at 4.2 K is fed to each coil individually. Helium exiting from the coils will cool the structural supports, leads, and the radiation shield at ∿ 100 K in the vacuum space. The total flow requirements are approximately 160 ℓ/hr for the entire machine. The superconducting field coil parameters are given in Table V.

The current collection system for the homopolar machine impacts the design to a high degree. The main machine design parameters affecting the current collection system are listed in Table VI.

TABLE V

SUPERCONDUCTING FIELD COIL

Coil size	6.35 cm (2.5 in.) x 116.8 cm (46 in.)
	2.46 m (97 in.) average diameter
Ampere-turns	10.35 x 10^6
Overall Coil Current Density	13 950 A/cm^2 (90 000 A/in.)
Filling Factor	0.6
Thermal Margin	0.6
Conductor Current Density	32 250 A/cm^2 (150 000 A/in.^{2})
Peak Field	85.6 kG
Energy/Coil	127 MJ
Average Radial Pressure	19.5 x 10^6 N/m^2 (2828 psi)
Axial Side Force	88.1 x 10^6 N (19.8 x 10^6 lbs)
Conductor Wt/Coil	3097 kg (6828 lbs)

TABLE VI

PARAMETERS AFFECTING CURRENT COLLECTION SYSTEM

Total Current	12.25 MA
Surface Velocity	277 m/s to zero
Magnetic Flux at Brushes	6 T axial, 1.5 T radial
Discharge Time	30 ms
Base Load Duty	3×10^6 pulses/yr
Machine Efficiency	95%

These design parameters are exceptionally difficult on four main counts: (1) the total current is higher than that of any other machine ever built, (2) the brush rubbing velocity is higher than that of any other machine ever built, (3) the magnetic field strength at the brushes is higher than that of any other machine ever built, and (4) the ultimate duty required is essentially that of a base load plant. To a certain extent these conditions are mitigated by the very short pulse duration. The machine efficiency requirement of 95% implies total brush losses of less than 0.6%. From the machine requirements the main requirements for current collection are given in Table VII. These requirements have been evaluated in view of known work characterizing brushes for current density, operating speed, contact drop, wear rates, and friction coefficients. Figure 5 shows the machine current density versus speed plotted at three-millisecond intervals.

TABLE VII

CURRENT COLLECTION SYSTEM REQUIREMENTS

High-Current Density	> 15.5 MA/m^2
Low Total Voltage Drop	≤ 0.5 V/slipring
High-to-Low-Speed Operation	$\pm$ 277 m/s to zero
Low Friction Coefficient	< 0.18
Minimize Circulating Currents	< 1 V/slipring
Low Wear	$< 1.6 \times 10^{-5}$ mm/pulse
Effective Cooling	$\bar{T} < 100°C$

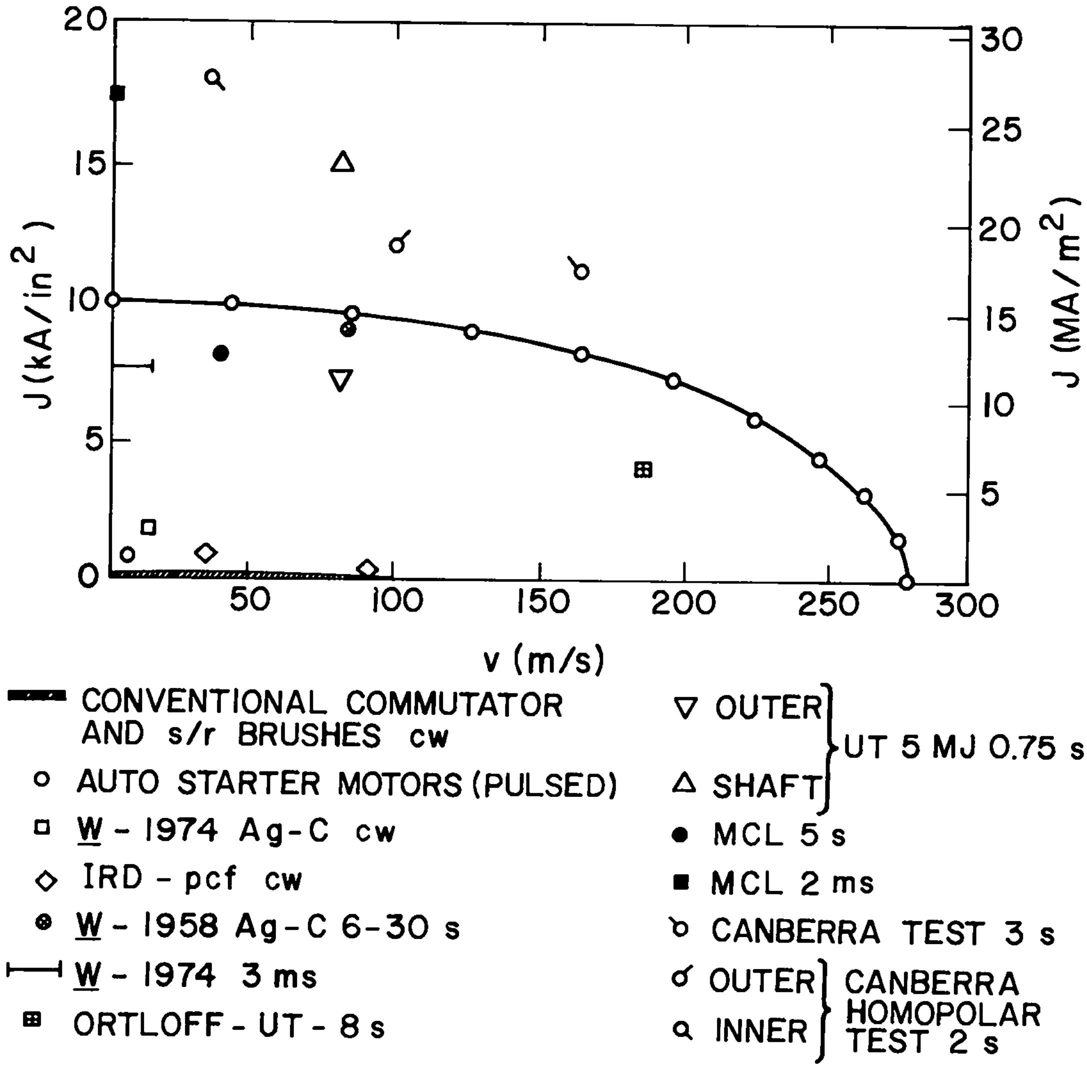

Fig. 5. Current Density - Speed Operating Experience.

One aspect of the machine operation is favorable in this respect, in that at the highest machine speed, the current is zero and only at low speeds is the current density high. The small shaded area on the lower left corner represents the traditional body of solid brush experience[15,16] and extends from about 200 A/in.^{2} to about 85 m/s. Also in the lower left corner are data points relating to continuous operation of plated carbon fiber brushes,[17,18] recent operating experience on continuous silver-graphite brushes,[19] and the most common use of brushes in pulsed operation, i.e., automobile starter motors.[20] The majority of the remainder of the figure was generated in connection with the Canberra homopolar generator program at the Australian National Laboratory; however, also included are data obtained at the University of Texas[21,22] and at Westinghouse.[23,24] Some of the data are also from pulsed testing for the Canberra homopolar generator.[20,25,26,27] Contact potential, wear rate, and friction data are available from the same references. The information relating to speed and current density operation is fairly encouraging in that it shows that the operation of the machine under consideration here is not too far removed from the range of prior experience. Contact potential results, Fig. 6, are also promising, showing voltage drops of about 0.5 V have been achieved in several experimental tests, albeit in many cases at contact pressures appreciably higher than are being considered here (16 psi). The wear rate data are not as satisfactory since most of the speeds and/or current densities were too low and the Canberra results had rates 7.5 to 300 times the present design levels but for sixty times longer pulse periods. This last area requires development. Noteworthy among the experimental wear rates is the very low value obtained with electrographitic grades in hydrogen.[28] Friction coefficients from the references are within the range of the present machine design.

A number of current-magnetic field interactions have been considered for the collector system. These include the basic I x B Lorentz force arising from the transport current and the homopolar field and radial fields giving rise to transverse brush voltages with associated transverse circulating currents. The latter problem is resolved by use of multiple sliprings angled to match the magnetic field directions. A schematic is shown in Fig. 7 together with plots of forces on the brushes.

Of the collector system functions, the brush constraint, feed, radial flexibility, and actuation are all influenced by the forces which act on the brushes. These forces may be divided as follows:

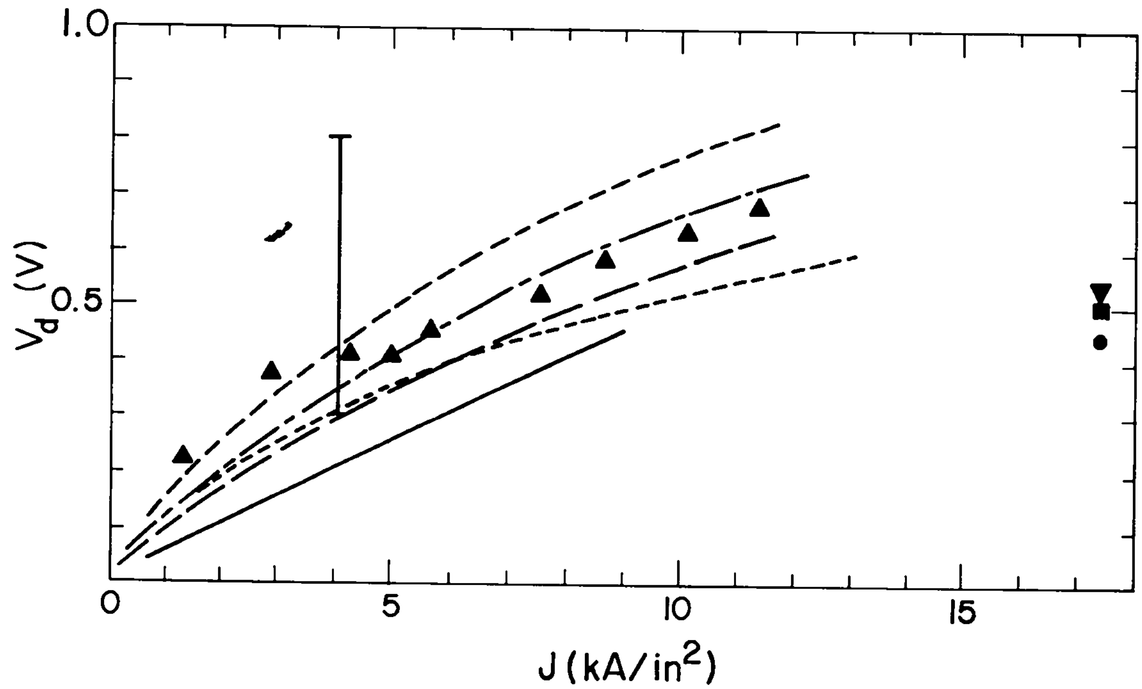

I	ORTLOFF	25 TO 170 m/s	5 GRADES	ON STEEL	20 psi
— —	MARSHALL	40 m/s	CMIS	ON STEEL	50 psi
-·-·-	MARSHALL	40 m/s	CMIS	ON STEEL	38 psi
- - -	MARSHALL	163 m/s	CMIS	ON STEEL	50 psi
——	W-1958	85 m/s	Ag-C	ON COPPER	20 psi
▲	CANBERRA	100 m/s	CMIS	ON STEEL	50 psi
-----	MARSHALL	167 m/s	CMO	ON STEEL	50 psi
● ▼ ■	MCL	ZERO	CMO, CMIS, CM2	ON STEEL	60 psi

Fig. 6. Contact Drop Characteristics.

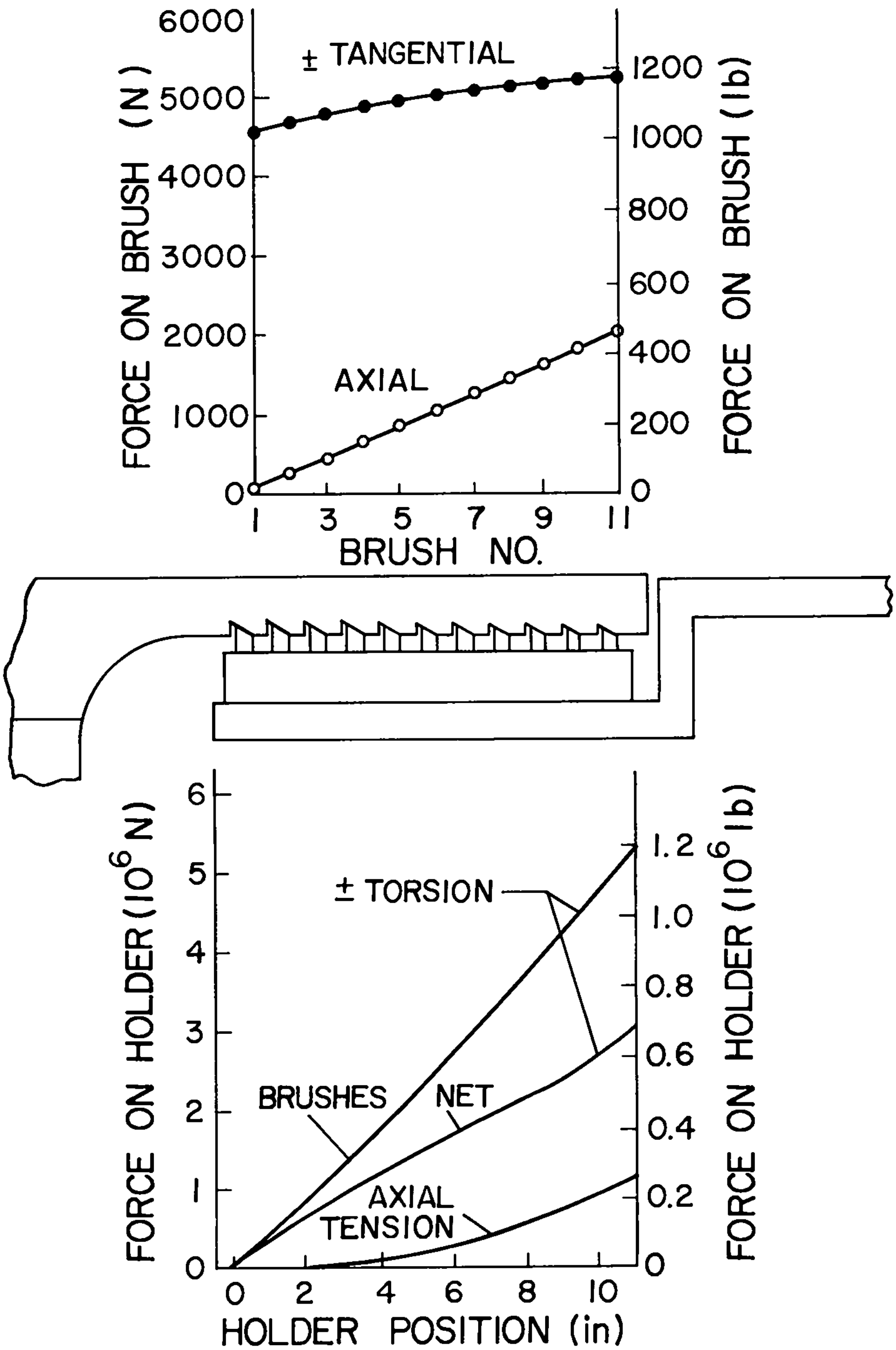

Fig. 7. Load-Current Forces (3-Inch-Long Brushes at 11 610 A/Brush).

Electrical Forces: Axial field/current interaction
Circumferential (self) field/current interaction
Shunt support loading
Current constriction
Circulating current/field interaction

Mechanical Forces: Slipring friction
Holder friction
Radial acceleration to follow slipring
Spring loading
Actuation loading (fluid pressure and acceleration)

Figure 8 shows the major forces acting on the brush. The axial-field/load-current interaction force is circumferential and acts against the direction of the rotor acceleration. During the slow-down cycle the direction of this force is the same as the velocity of the rotor (and brush friction force), but during the start-up cycle (reversed speed) the brush force is opposite to the direction of the rotor velocity. The circumferential-field/load-current interaction force varies with the brush row, with the highest force acting on the brush row which is innermost in the load current loop, and the direction of this force is axial (for radial brushes) and outward from the current loop. Figure 7 shows the initial estimates of maximum load-current forces, for a 1.78 x 4.23 cm (0.7 in. x 1.66 in.) brush cross section and a 7.62 cm (3 in.) brush length. The "net" torsional load on the holder shows the effect of axial current flow in the holder, which interacts with the radial field to induce a torque counter to that of the brushes. The shunt loading of the brush can be significant but the magnitude cannot be determined until the system configuration is defined. In addition to the primary electrical forces on the brushes due to discharge current, there are secondary brush forces which result from the magnetic field being nonuniform in the brush region. Since the axial component varies with radius, any radial brush motion during actuation or discharge will induce circumferential eddy currents which, coupled with the field, result in an opposing or damping force. The eddy current force varies from brush row to brush row due to differences in gradient of the magnetic field. The axial field is plotted versus displacement, z, from the center of the superconducting field coil for both inner and outer brush radii in Fig. 9. The several forces were combined including consideration of motions of the rotor with circumferential growth and slipring eccentricity arising from the spokes. A conceptual schematic of the resulting brush with some of

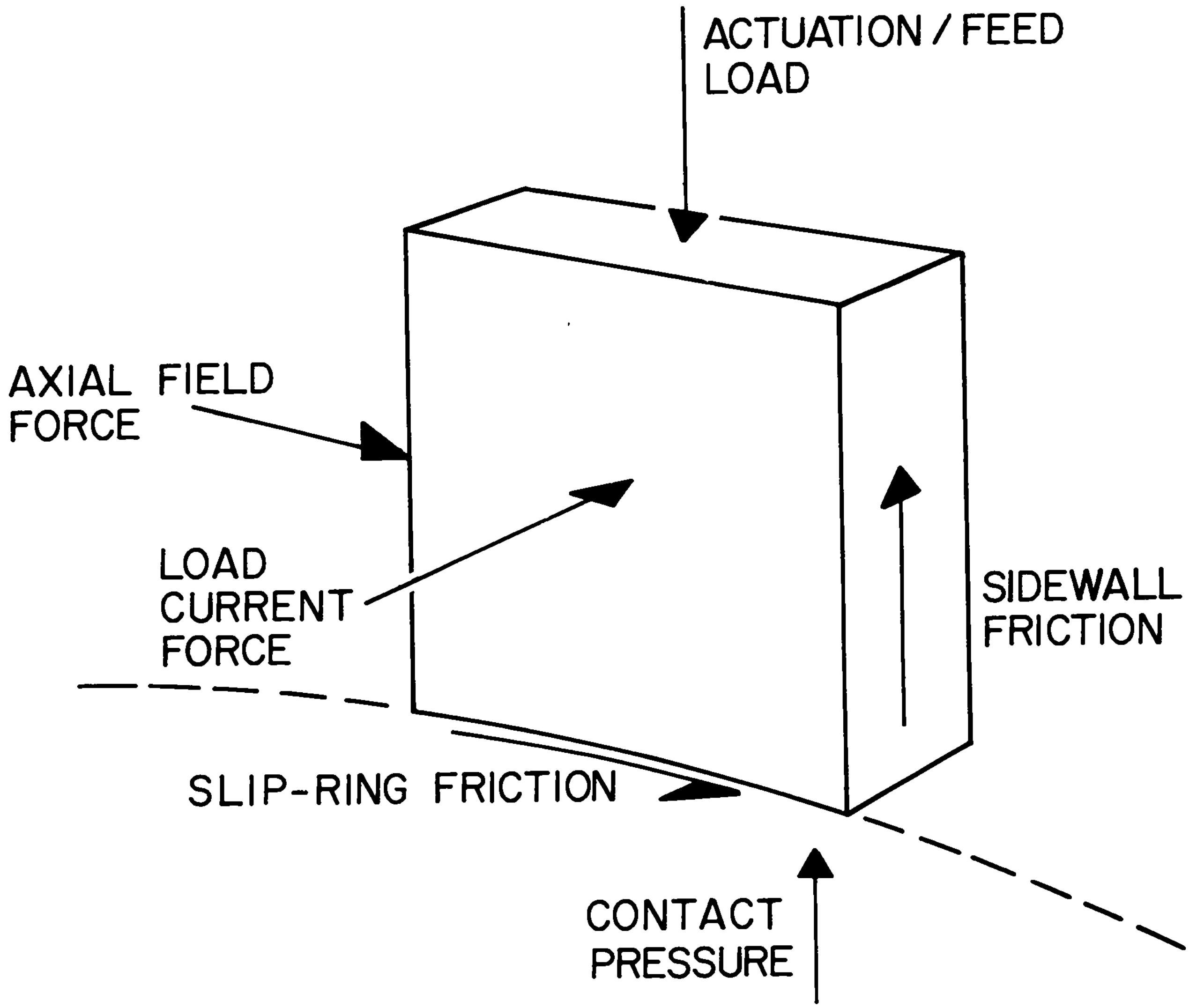

Fig. 8. Major Forces Acting on Brush.

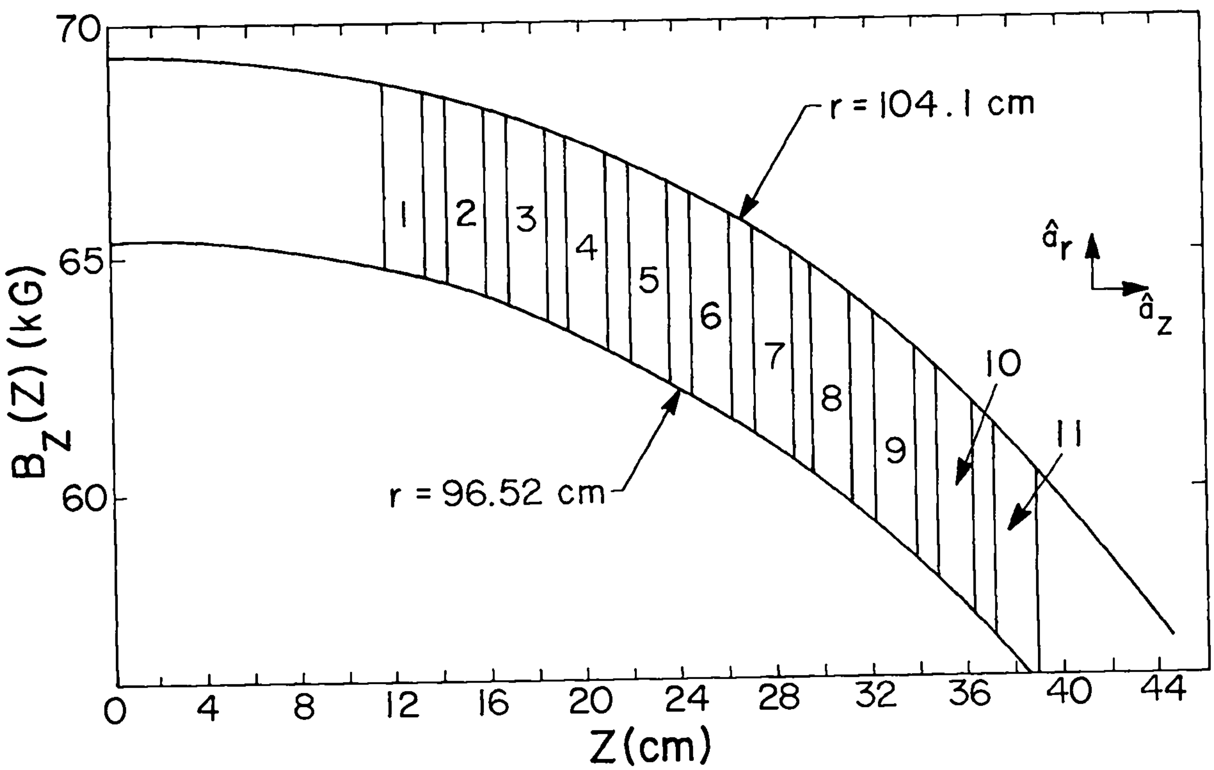

Fig. 9. Axial Magnetic Field in Brush Region.

the functional provisions indicated is shown in Fig. 10. The pivoted-sleeve brush holder permits a limited radial motion with low friction and allows brush feed relative to the holder to accomodate wear when the magnetic forces are removed. In a typical cycle, the brushes are actuated at maximum rotor speed. The pivoted-sleeve remains centered by light springs. During the subsequent discharge cycle, as the load-current increases, the magnetic force locks the brush to the sleeve and this assembly moves radially inward with little mechanical resistance as the slipring diameter contracts and the rotor stops. During the "burn" period, the magnetic forces are eliminated, so that the sleeve may return to its centered position. In the start-up period, the brushes immediately lock up and the brush/sleeve assembly moves out radially as the slipring diameter grows. Another feature is a possible means to position the face of the brush at the same retracted position independent of brush length due to wear. It is proposed that retraction of the brush by means of gas pressure difference would expose ports that would balance the force across the brush by allowing leakage into the vacuum chamber.

This section has reviewed the important features of the 1.3-GJ RTPR homopolar machine design. Since one aspect of the contract responsibility with EPRI has been to provide a conceptual, full scale machine design to guide the detailed design of a model machine, this portion of the work is complete.

B. Model Machine Design

The full scale homopolar machine provides the basis for the model machine design, fabrication, and testing. Choice of size for the model homopolar is predicated upon certain judgment factors which call for as small a machine as possible to minimize cost and to prevent using extraordinary machining practices and at the same time sufficiently large to establish an advance in the state of the art to prove a number of significant developments for the large machine. Implicitly associated with these judgments is the need to build and test a meaningful homopolar in the near future at a reasonable cost. The characteristics established to model the full scale homopolar are as follows:

a. Same current density in brushes as full sized machine (1.55 kA/cm^2).
b. Same rotor peripheral velocity (277 m/sec).
c. Machine atmosphere of pressurized hydrogen (3 atm.).
d. Superconducting field coils of NbTi at as high a field as possible.
e. More than one row of full size brushes at each collector area.
f. Two counter-rotating rotors.
g. 30-ms discharge time.

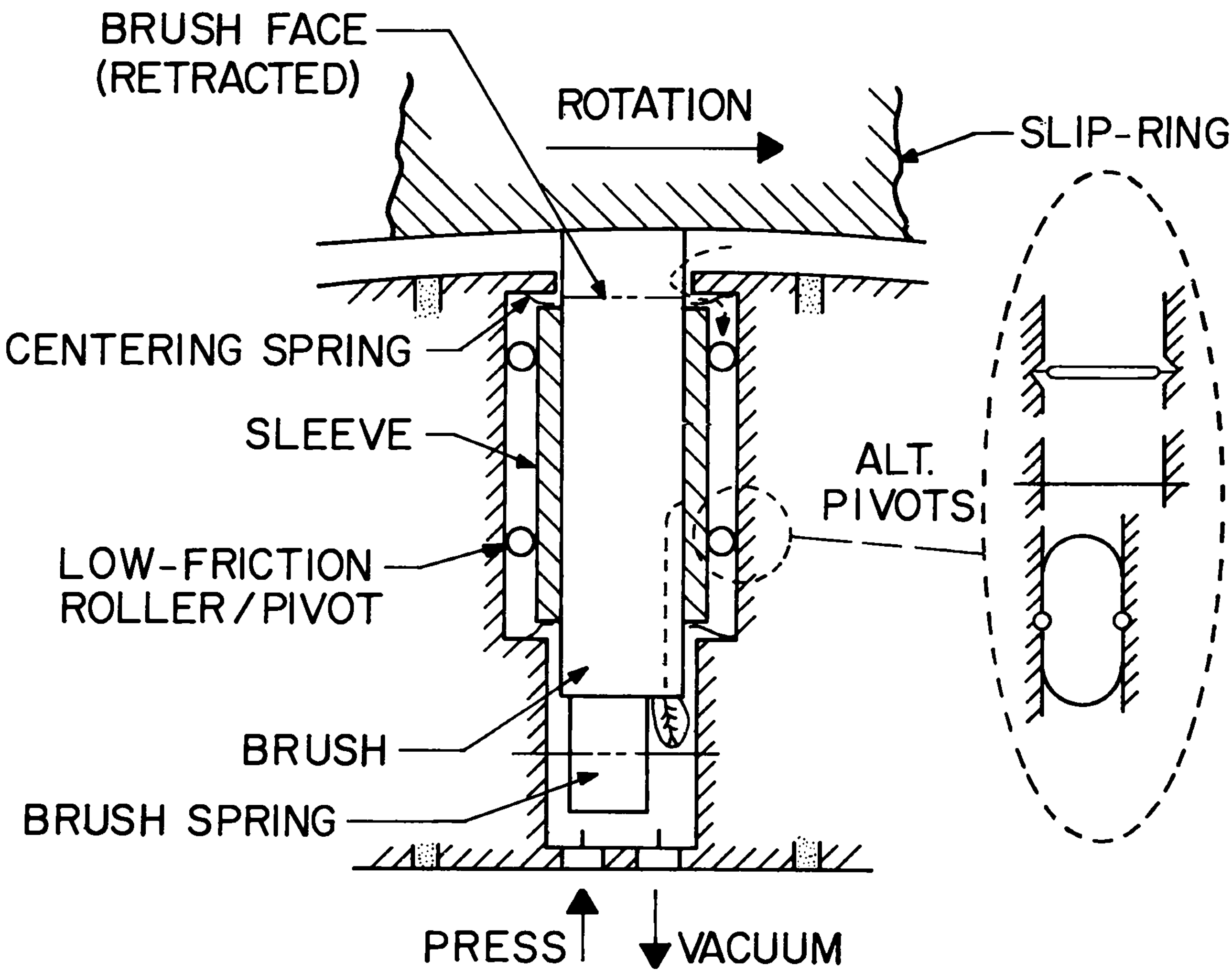

Fig. 10. Current Collection System Concept.

h. Oil film bearings.

i. Use readily available structural materials.

The model size was chosen at one-third the full scale machine based upon dimensions. A somewhat smaller machine would not provide adequate space for full scale brushes.

The same peripheral rotor velocity at one-third rotor diameter, one-third the rotor length, and one-third the rotor drum thickness reduces the energy stored by a factor of one-third cubed. Going from four pairs of counter-rotating rotors to one pair decreases the energy stored by another factor of one-fourth. Use of the NbTi superconductor decreases the average field somewhat to provide a 10-MJ model homopolar. The dimensional scaling features are shown in Fig.11 at the full scale machine average field of 3.0 T.

Since the design problems for the 1.3-GJ·homopolar have been discussed in detail in the previous section and are generally similar but changed in degree for the 10-MJ model machine, they will not be covered here again except to state how they have been resolved if the approach is unusual. For this reason the section mostly treats the preliminary scaled homopolar characteristics with the awareness that efficiency, fatigue life, electrical design, mechanical and thermal analysis, stress analysis, rotor dynamic studies, superconducting field coil, and current collection system are all given proper consideration. At the time of this proposal the EPRI study contract is still under way; hence, the final 10-MJ design detail may be altered somewhat from that presented herein.

Two significant changes have been incorporated into the model machine design. These are the abandonment of a spoke supported rotor drum in favor of a disc supported drum and the use of a thin brush. The spoke rotor design would not provide brush access through the rotor in the model machine since it is dimensionally too small. This leaves the question of brush access in the large machine unanswered since we do not address the problems associated with the spoke attachment in the model machine. If the spoke is made of sufficiently strong aluminum alloy, it would have a short life due to notch and crack sensitive fractures of the material. The disc supported rotor drum design meets acceptable stress levels with aluminum alloys which are not crack sensitive. The brush design was changed to a circumferentially thin brush with an approximate aspect ratio of seven instead of a nearly square brush. This is necessary to reduce the radial lifting force arising from interaction of transverse currents and the excitation field. These brushes are mounted in clusters of twenty with a single hydraulic actuator.

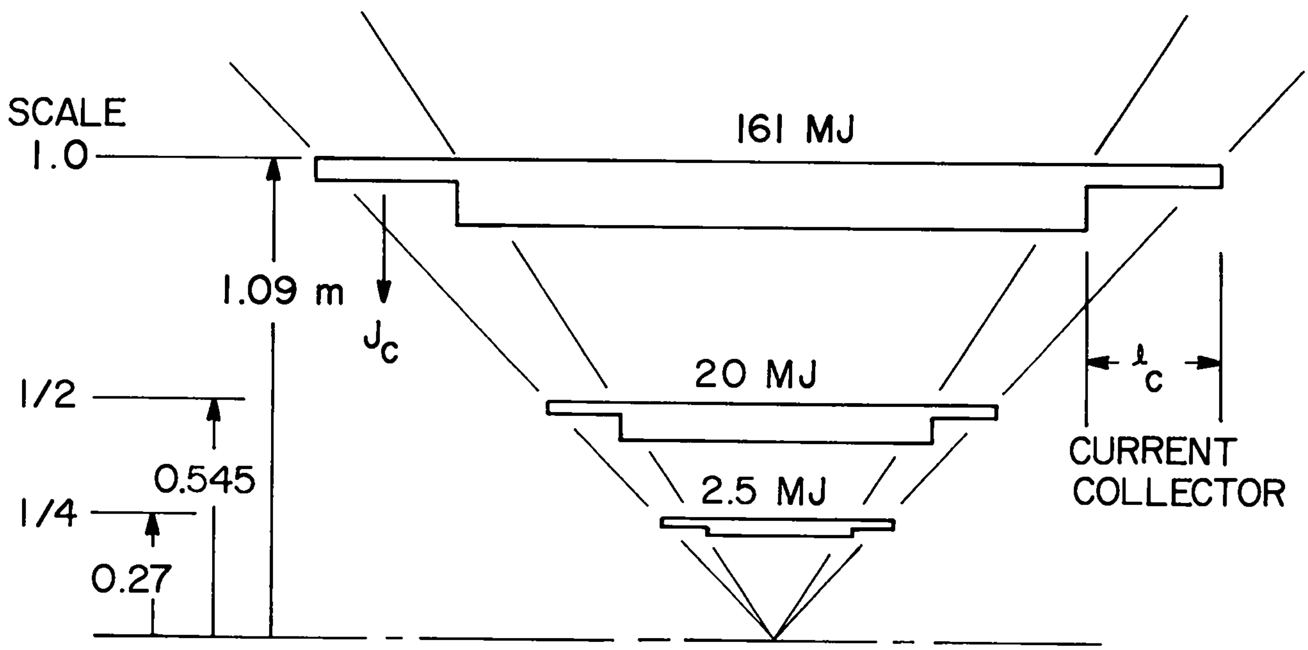

v = TANGENTIAL VELOCITY - 277 m/s

J_c = COLLECTOR CURRENT DENSITY (AVE) - 730 A/cm^2

T = DISCHARGE TIME - 30 ms

B = 30 kG (AVE)

Fig. 11. Rotor Scaling.

The electrical characteristics for the 10-MJ model homopolar, in addition to those prescribed to scale the full size machine, are given in Table VIII, and the scaled dimensions are given in Table IX.

Stress analysis is routine for most of the model machine and the design is straight forward. The rotor is a region of high stress and has been examined for several detailed disc supported concepts which will use 7005 Al alloy with stresses up to 16 ksi and deflections of 0.012 in. on the drum. Slipring stresses and deflections are higher and require banded strengthening on the outside circumferential surface to diminish bellmouthing.

All the vibration modes of the full size homopolar were also examined for the model. The rotor critical speeds safely exceed the operating speed if the bearings are made sufficiently stiff.

Preliminary bearing design calls for a full arc journal bearing with a 6.5-in. diameter, 0.006-in. radial clearance, and length-to-diameter ratio of 0.25 using PDS 9802 turbine oil. Rotor shaft transient displacement in the bearing is less than 0.001 in. during machine discharge. The bearing diameter can probably be reduced pending final rotor shaft size determination. This is

TABLE VIII

10-MJ MODEL HOMOPOLAR ELECTRICAL CHARACTERISTICS

Peak Voltage	719 V
Peak Current	$1.5(10)^6$ A
Average Radial Field Between Collectors	22.8 kG
Average Axial Field Within Collectors	
Center	41.0 kG
End	36.8 kG
% Flux Leakage	45.9%
Peak Fields	64.5 kG
Superconductor Weight	883 kg (1946 lbs)
Total Coil Energy	8.12 MJ
Total Amp-Turns	7.25×10^6
Total Magnetic Iron Weight	
With 3-in.-Thick Outer Shield	20 400 kg. (45 000 lbs)
With Optimized Outer Shield	17 500 kg. (38 500 lbs)

TABLE IX

10-MJ MODEL HOMOPOLAR DIMENSIONS

Overall Diameter	2.286 m. (90 in.)
Overall Length	2.108 m. (83 in.)
Rotor Diameter (At Peak Speed)	0.721 m. (28.4 in.)
Single Rotor Length	0.701 m. (27.6 in.)
Rotor To Rotor Centerlines	0.742 m. (29.2 in.)

dependent upon the required gaseous H_2 coolant channel and instrumentation leads through the center of the shaft. Reduction of the bearing dimensions will decrease losses which are disproportionately large since the bearings do not scale down directly from the 1.3-GJ homopolar.

The superconducting field coils for the model machine are to be intrinsically stable and will be divided into three major sections located centrally in the machine outside the stator and over the region of the brushes contacting the rotor sliprings between the two drums and similarly over the brushes contacting the sliprings on the outside ends of the rotors. This arrangement provides a field configuration most nearly perpendicular to the rotor drum and parallel to the brush-slipring contact surfaces. The perpendicular drum field maximizes the current generation and the parallel contact surface field minimizes circulating brush currents. The field coils will operate with a maximum field on the conductor of 64.5 kG. The rectangular, monolithic, multifilament, twisted superconductor will carry 1-kA transport current and have a Cu to NbTi ratio of two. The design operating point for the superconductor is 80% of j_c at 64.5 kG and 10^{-12} ohm-cm resistivity. This provides a 1.0 K thermal margin. The coils are to be connected in series. The design provides for an open vented structure with pool immersion in ℓHe and cooling channels having electrical insulation between winding layers. Coil parameters are given in Table X.

An a.c. loss analysis during energy transfer has been made. The major effect arises from rotor growth of 0.020 in. on the radius. Both the stator and thermal radiation shield in the coil dewar serve as eddy current shields. The a.c. radial magnetic field will sweep from zero amplitude to +50 G at 30 ms and to -50 ms at 120 ms for a typical RTPR discharge-recharge cycle. The a.c. axial magnetic field component is slightly smaller and lags by 20 ms. The temperature

TABLE X

SUPERCONDUCTING FIELD COILS

	Center	End
Cross section	8.12 cm x 38.96 cm (3.197 in. x 15.34 in.)	8.12 cm x 25.15 cm (3.197 in. x 9.9 in.)
Average Diameter	0.875 m (34.46 in.)	
Overall Current Density	10,000 A/cm^2 (64,500 $A/in.^2$)	
Filling Factor	0.6	
Conductor Current Density	16,667 A/cm^2 (107,500 $A/in.^2$)	
Conductor Current	1000 A	
Peak Field	64.5 kG	
Energy Stored	3.738 MJ	2.189 MJ
Ampere-Turns	3.163×10^6	2.041×10^6
Average Radial Pressure	12.6×10^6 N/m^2 (1829 psi)	12.5×10^6 N/m^2 (1816 psi)
Axial Compression	7.96×10^6 N (1.79×10^6 lbs)	2.60×10^6 N (0.585×10^6 lbs)
Net Axial Thrust	0	3.74×10^6 N (0.84×10^6 lbs)
Conductor Weight	385.4 kg (849.6 lbs)	248.7 kg (548.3 lbs)
Total Inductance	16.2 H	

rise is 0.2 K from an estimated 0.2-kJ energy deposition. Further analysis is required to determine magnetic flux flow heating from machine vibration.

A coil quench study indicates the energy stored in the field can be safely released to an external dump resistor. Pertinent factors from the study are given in Table XI.

The major structural forces on the coils are the basic hoop stress and $I \times B_r$ axial forces associated with distributed solenoids. Other forces arise from misalignment of the rotor and transient effects. The hoop stress is constrained within the ℓHe dewar with a retaining ring of 310 stainless steel. Table XII gives the details of the ring design. The axial forces can also be entirely constrained within the ℓHe dewar, if there is no misalignment, with structure

TABLE XI

SUPERCONDUCTING COIL QUENCH FACTORS

External Discharge Resistor	2.0 Ω
Internal Resistance (At 4.2°K)	0.5 Ω
Time Constant	6.5 s
Peak Radiation Shield Pressure	200 psi
Peak Radiation Shield Current Density	45 000 A/in^2
Radiation Shield Resistivity	2×10^{-7} Ω-cm

provided between the coils. Segmented structural support in the individual coil windings is also provided to take the axial load within the coils. Misalignment of the coil can create some additional forces. These must be removed by low thermal conductivity structural supports to the ambient temperature dewar wall. The parameters for the axial force structural members between the coils are given in Table XIII.

TABLE XII

SUPERCONDUCTING COIL RETAINING RING

Internal Magnetic Pressure	1829 psi
Retaining Ring Design	
Material	310 sst*
Inside Diameter	37.66 inches
Thickness	1.6 inch
Hoop Stress	24450 psi
Radial Deflection	0.015 inches
Retaining Ring Thermal Design	
Coil Contraction	0.0546 inch
Ring Contraction	0.049 inch
Initial Shrink (Radial)	0.0055 inch
Initial Ring Coil Pressure	510 psi
Initial Ring Stress	5500 psi

*Allowable Stress = $\frac{2}{3}$ Syp = 70,000 psi.

TABLE XIII

SUPERCONDUCTING COIL AXIAL SUPPORT STRUCTURE

Axial Force Between Magnets	0.84×10^6 lbs
Axial Structure	
Thickness	0.560 inches
Tensile Stress	15 000 psi
Axial Deflection	0.006 inches
Bolted Connection	
No.	93
Size	0.625
Load/Bolt	9000 lbs
Bolt Stress	43 000 psi

A single annular ℓHe coil dewar is used with breaks in the dewar between coils to provide for support of the iron located adjacent to the stator and between the coils. Two 1.0-kA, cryogenic leads are required. The dewar is supported from the external iron flux shield with tie rods. The radial load is determined by the mass of the dewar and coils and the axial load by an assumed misalignment force of 10% of the axial force between the coils. The tentative tie rod design details are listed in Table XIV. The natural frequencies calculated in this first design of the tie rods are too low, being below the homopolar operating speed, and could give rise to coil vibration. A redesign to a higher frequency or highly damped tie rod is in order. The estimated dewar heat load is given in Table XV. Although these values appear to be low, they are based, in part, upon Westinghouse experience with the 5-MVA superconducting generator made by them. A factor of two or three error in these values is tolerable.

Brushes and the current collection system for the model homopolar have already been mentioned. Four rows of brushes will be used on each end of the rotors to mockup the current collection system. The peak brush current will be 1.55 kA/cm^2. Dimensional details for locating the brushes in the homopolar are given in Table XVI. The table references the axial position of the brushes with respect to the conical bearing support structure which appears as an "A-frame" in sectional view, see Fig. 3. The angle is that of the brush-slipring contact surface designed to match a constant field line to eliminate circulating currents. The field components at the contact surface are also included in the table.

TABLE XIV

SUPERCONDUCTING COIL DEWAR TIE RODS

Radial Design Force (Cold Weight)	3000 lbs
Radial Structure	
Material	Invar
Rod Diameter	0.25 inch
No. of Rods (Each End)	4
Design Stress (2/3 Syp)	61 000 psi
Radial Spring Constant	0.84×10^6 lbs/in
Radial Natural Frequency	2500 rpm
Axial Design Force (10% Of Inner Magnet Force)	84 000 lbs
Axial Structure	
Material	Inconel 750X
Rod Diameter	0.625 inches
No. of Rods (In Each Direction)	3
Design Stress (2/3 Syp)	87 000 psi
Axial Spring Constant	0.5×10^6 lbs/in.
Axial Natural Frequency	2 750 rpm

The EPRI contract work is to be completed late in CY1976 and concluded with an engineering design of the one-third scale, two-rotor homopolar capable of storing 10 MJ of energy with a peak current of $1.5(10)^6$ A and peak voltage of 719 V with a 30-ms discharge time. The program proposed here is to complete the manufacturing drawings for the model homopolar, manufacture the homopolar, design and build test facilities for the machine,and thoroughly test the homopolar machine.

TABLE XV

SUPERCONDUCTING COIL DEWAR HEAT LOAD, WATTS

Source	Center	End
Structural	0.0	1.4
Radiation	0.13	0.13
Leads	0.50	0.0
Residual Gas Conduction	0.30	0.30
Total	0.93	1.83

TABLE XVI

CURRENT COLLECTION SYSTEM

Centerline Distance Brush to A-Frame cm (in.)	Centerline Radius cm (in.)	Angle	Radial Field (kG)	Axial Field (kG)
Center Sliprings:				
3.23 (1.27)	34.940 (13.756)	4.0	3.9	56.1
6.02 (2.37)	34.402 (13.544)	8.6	8.3	55.2
8.81 (3.47	34.551 (13.603)	14.5	13.8	53.4
11.6 (4.57)	34.417 (13.550)	19.3	17.7	50.7
End Sliprings:				
3.23 (1.27)	34.714 (13.667)	8.2	-7.0	-49.1
6.02 (2.37)	34.435 (13.557)	2.8	-2.5	-51.0
8.81 (3.47)	34.435 (13.557)	-2.7	2.4	-51.7
11.6 (4.57)	34.714 (13.667)	-7.9	7.1	-51.2

V. PROPOSED PROGRAMS

The 10-MJ, 30-ms discharge model homopolar machine represents a number of advances in technology each of which must be successful to achieve the projected machine performance. Because of the features incorporated into the machine which tax existing technology, it is necessary to conduct a component development and testing program in parallel with and even prior to the completion of the design through the creation of the manufacturing drawings. This section deals with the machine construction-component fabrication and testing, completion of the manufacturing drawings, construction of the actual 10-MJ machine; preliminary testing of the machine at Westinghouse; and the LASL facility and tests.

A. Machine Construction

The technical requirements of the 10-MJ homopolar will be provided for in the detailed engineering design. This must be converted to manufacturable design using the results of required component and process developments. The construction program will be conducted in the following general sequence.

1. Convert detailed design drawings to manufacturing drawings using the results of component development of the brush loading system, aluminum rotor, and superconducting windings and of process development for the bearings, stator conductor, crossover assembly, metal joining, and miscellaneous subcomponents.
2. Construct and test components in accordance with the drawings.
3. Assemble the stator system.
4. Assemble the entire machine.
5. Construct and test auxiliary components and systems.
6. Test the machine.

Several major components of the 10-MJ machine require development and testing prior to completion of the manufacturing drawings and to the construction of the complete machine. These are the solid brush current collection system, the superconducting magnet, and the aluminum rotor. The development programs for these components follow.

Functionally, the current collection system provides brush constraint, current transfer, loading on the slipring, and brush lifting. In addition to the copper-graphite brushes the principal components of the current collection system include the brush holders, current shunts, interconnections, actuators, and hydraulic actuator supply. The holders constrain the brushes in the circumferential and axial directions and permit radial sliding to accommodate brush wear and slipring radial growth. The shunts transfer the current from the brush to the holder assembly by sliding contact spring-type fingers attached to the holder. The interconnections are transposed and cross-connect the brush holders of adjacent rotors to eliminate voltage gradients and circulating currents. The hydraulic actuators load the brushes on the slipring and lift the brushes between current pulses by means of a hydraulic supply distribution and control system. The approach to the development will be to progress from testing of single actuator brush assemblies through testing of a complete assembly.

The ability to control the brush load and minimize electrical losses are prime considerations in the development of the holder and current shunt. Due to the electromagnetic side load on the brush it is desirable to minimize the friction coefficient between the brush and the holder wall. The force between the brush and the sliding contact shunts is also reflected as a radial load by the friction coefficient at the contact surface.

The objectives of development are to minimize the effects of side load and friction on the radial flexibility of the brush. Further, the electrical contact resistance between the sliding contact shunts and the brush must be minimized with modest contact forces. A series of experiments will be conducted to explore the effects of brush material and surface treatment of the brush, holder, and contact fingers to minimize friction and contact drop while obtaining high resistance to welding effects and side wear.

Precision is required in the timing of the brush loading action as affected by the stroke, compliance in the structure, supply pressure, stroke velocity, friction, pressure drops in the control lines, etc. Since there are prospects of initial bouncing and circulating current flow as the brushes are loaded on the slipring, this potential problem requires selection of velocity-time and pressure-time profiles. Single loader systems will be constructed to establish the loader characteristics. Synchronization of multiple loaders will also be studied.

Variations in the slide motion between the brush and slipring adversely influence the transfer of electrical current. Sliding instability may be induced by the frictional characteristics of the contact materials themselves, by external forces transmitted through the support mechanisms, or by aerodynamic lift which reduces the ability of the brushes to follow the collector surface. Operation of brush assemblies on high-speed collector rings will permit the investigation of both the natural frequencies in the complex structure and their damping requirements.

The rotor is to be a conducting aluminum alloy drum with sliprings on each end. To reduce radial drum growth and to maintain acceptable stress levels during acceleration and deceleration, internal tapered reinforcing discs are used. The support is provided by an internal hollow shaft 6.5 in. in diameter. The shaft also acts as the rotor journals. The disc rotor assembly is shrunk onto the central hollow shaft. The sliprings at the ends of the drum must be plated with copper for acceptable brush wear. A carbon-fiber reinforced plastic retaining ring is to be placed over the slipring region to minimize slipring deformation.

The rotor design must be mechanically stable, precisely balanced, and have a small runout. The rotor drum must have circumferentially equal axial electrical conductivity to prevent large a.c. losses. The development of a rotor that meets the design objectives requires process development.

The presently conceived fabrication procedure includes the use of six discs joined at the o.d. and i.d. to form the rotor. The discs are to be made of forged aluminum alloy 7005. Four of the discs will be similar with two end discs with the slipring surfaces.

Three critical processes are required to be developed successively to achieve a sound rotor design.

The outer joint bond of the rotor discs must be uniform electrically to insure even distribution of axial currents. Several metal joining options - brazing or diffusion bonding of either the inner and outer joints and electron beam welding of the outer joints - are under consideration for selection. The development of the joints will progress from small mockups to full size mockups. Successive bonds will be evaluated until satisfactory joints have been achieved for both inner and outer cylinders. The quality of the mockup joints will be verified by nondestructive examination developed for the machine rotors and by sectioning.

The slipring reinforcement will utilize a carbon fiber-epoxy band to be applied over the slipring extension in several separate bands. The process for banding must be developed and tests conducted to determine the adequacy of the bands under operating conditions. A procedure must be developed to prevent loosening during curing of the epoxy matrix due to differential thermal expansion. This is normally achieved by a double cure cycle in which an initial matrix to fiber band is formed at low temperature that will prevent fiber redistribution during curing. The final cure at an elevated temperature will increase the fiber to matrix band to a level required for the design properties.

The sliprings will be plated with high density copper to provide an excellent metallurgical bond with good electrical conductivity. The plating must be achieved without pitting or corrosion of the aluminum structure. Basic processes for plating 7005-F aluminum with copper have already been developed.

Once these processes have been evolved an assembly sequence for the rotor must be developed and successfully demonstrated by building a test rotor prior to the fabrication of the rotors for the machine.

During the rotor construction careful inspection will be conducted to ensure that the discs are sound and have no serious flows, the metal joining meets the established standards, and the banding system is sound. Balancing of the rotor is extremely important and provision will be made for this in the detailed design.

The rotor will be tested at various speeds up to full speed to determine run out, growth, and mechanical stability. Finally it will be run at 110% of design speed to measure strains and dynamic characteristics. Following these tests, the test rotor will be destructively tested to determine joint strength, banding properties, and slipring plating adequacy.

The superconducting coils for the field excitation system consist of three magnets mounted on a common cold structure. These coils must operate with a high degree of reliability. In the event of a quench (loss of superconductivity), the energy and helium gas discharge must be arranged so that no detrimental effects will occur.

Superconducting coils of about the same size and characteristics as those proposed have been built. The energy stored in the proposed magnet exceeds that of previous magnets of a similar kind.

To establish an adequate base for the field coils, it is proposed first to design, build, and test the center coil of the machine as a prototype. The end coils will then be built after successful development of the first coil.

Testing of the first coil will verify the adequacy of the design considerations for the superconductor specifications; the cooling system and heat transfer analysis; thermal, mechanical, and magnetic stability of the winding; quench sensing and associated energy dump; electrical leads; helium system and dewar; and coil structural support.

The design of superconductor is a key part of the magnet development process and the selection must consider stability, conservative a.c. loss estimates, and charging losses. The design parameters to be selected include filament diameter, twist pitch, aspect ratio, and filament distribution in the copper matrix.

A number of tests and observations will be made to evaluate the superconductor. The performance of the conductor will be verified by short sample stability, and a.c. loss testing, and suitable mechanical testing. A physical inspection will determine conductor dimensions and their variation along the length, together with filament size, number of filaments, filament distribution, filament aspect ratio, and the distribution of the matrix over the cross section. Electrical measurements will be made to obtain the j_c versus H curves for appropriately selected samples. These measurements will be performed at various field orientations to measure the anisotropy due to the rectangular configuration. The insulation will be examined for flaws and uniformity of application.

To simulate actual operating conditions and perform the necessary development tests on the first superconducting magnet several pieces of equipment will be needed. These include a dewar, power supplies, and protective circuitry to include current sensing capability and switchgear.

Prior to shrink fitting and welding the support structure and compression pads into place, a test will be run to establish the capability of the coil to function as a superconducting magnet and to assess joint and lead-in quality. The dewar for this test can subsequently be converted into the vacuum vessel required to contain the completed coil with the support structure welded into place.

A direct current source, capable of delivering 1 kA at up to 10 volts, at a controllable rate, will be required to establish the d.c. steady state field. An a.c. supply of appropriate frequency will be needed to supply up to 5-A peak current to be superposed on the d.c. to simulate a.c. coupling fields.

Protective circuitry is needed to test the coil with a current sensing system to detect a change in the d.c. field current as an indication that a quench has been initiated and to generate trigger signals for the switchgear. The switches will connect the protective circuit; disconnect the power supply; and remove, in a programmed time sequence, values of parallel connected resistors, so the total resistor value varies inversely with coil current during quench.

The following tests and measurements are planned for the prototype coil. Current will be increased at variable rates, to various current levels. Following the steady state operation test, an a.c. current will be introduced to the coil at various d.c. levels to evaluate losses. Measurements will be made of temperatures at various locations, helium consumption, current, field distribution, and forces.

A quench at low currents will be provided by a small heater attached to an exposed joint wire. Quenches will be induced at various current levels and measurements will be made to determine protective circuit capability, pressure, current versus time, temperature, helium requirements for cooldown after quench, and cooldown time after quench.

Manufacturing drawings will include machine and component drawings at all levels. Each drawing will specify dimensions, materials, process specifications and quality assurance requirements. Where process standards do not exist or are not easily defined, minor developments will be conducted to develop the processes required to conduct the component construction. These developed processes will be identified on the manufacturing drawings, so that the component and machine construction will be controlled at all times.

Manufacturing engineers from both the Westinghouse Electromechanical Division and the Research Laboratories will participate in this design phase to ensure that the drawings reflect the best approach to the component and machine fabrication.

The 10-MJ machine represents a complex assembly of precise components which must operate reliably as a system. The construction of the machine will progress through subcomponent and component assemblies to the overall machine assembly. Each subcomponent and component design must be verified by measurement or test before it can be moved to a higher level of assembly.

The main subassemblies of the machine will consist of the main stator system which in turn consists of

a. Main steel frame,
b. Superconducting magnets and cryogenic systems,
c. Stator return conductor, and
d. End closures;

the rotor support assemblies which contain

a. Brush loading systems,
b. Cross over connections, and
c. Bearing housings;

the rotors; and the control tube containing

a. Return gas flow,
b. Bearing lubricant lines,
c. Brush loading hydraulic lines, and
d. Sensor leads.

The auxiliary systems for the machine include the bearing lubrication system, the gas blower and heat exchangers, the hydrogen auxiliaries, and the brush loader hydraulic system. All of these main subassemblies will be constructed and tested separately prior to the complete machine assembly.

The construction of the machine will utilize Westinghouse facilities and several subcontractors. The locations have been and will continue to be selected on the basis of relevant experience, facilities, and cost. The major Westinghouse efforts will be assigned as follows:

Electro-Mechanical Division

a. Critical welding.
b. Precision machining.
c. Main stator assembly.
d. Precision balancing.
e. Vacuum testing.

Research and Development Center

a. Superconducting magnet winding and testing.
b. Machine assembly and testing.
c. Brush loading system development and construction.
d. Rotor structure process development.

B. Preliminary Testing

The preceding section on machine construction considered a number of developmental items and tests associated with these components and subassemblies. This section treats the preliminary machine testing as finished subassemblies and as an assembled unit.

The preliminary tests will be performed at the Westinghouse Superconducting Machinery Test Facility where a test stand, helium refrigerator, d.c. power supplies, and instrumentation are available. The test facility is designed for no-load testing of assembled machines as well as sub-assembly component testing without provision for pulsing or dissipation of large amounts of energy. The preliminary tests, based on the existing facility capability are designed to achieve the following objectives:

a. Sub-assembly performance test including stator assembly, brush actuation gear, and rotors.
b. Establish machine assembly and alignment.
c. Establish machine dynamic characteristics over the entire speed range.
d. Establish brush actuation system performance.

e. Evaluate atmosphere control and cooling system.

f. Determine performance characteristics to insure proper machine operation at LASL pulse test facility.

g. Establish operating procedures for all subsystems, instrumentation, and data gathering systems.

h. Establish assembly and disassembly procedures.

Prior to machine assembly the stator must undergo tests to insure proper operation. The primary area involves operation and alignment of the magnetic system. The stator will be evacuated and inspected for vacuum leaks. Following the vacuum leak test, the superconducting windings will be cooled down to 4.2K and the low temperature region losses will be determined to verify refrigeration requirements. The entire three-coil superconducting field winding will be excited to evaluate charging rate capabilities, refrigeration load, and steady state operating procedures. After satisfactory completion of these tests a quench will be initiated to check detection devices and to be sure that the coil protective system is functioning correctly for the three-coil assembly.

Axial and radial alignment of the magnetic field in the machine bore will be required to eliminate the effects of tolerance accumulation during stator assembly. The machine design has provisions for alignment of the superconducting field coils while at operating temperature. The adjustment must be accomplished at full field to eliminate field distortion due to nonsaturated iron that would otherwise occur at reduced excitation levels.

The stator conductor d.c. resistance and the ground wall insulation integrity will be measured.

The entire brush actuation system, supply system, and diagnostic instrumentation will be assembled with dummy sliprings for pre-assembly testing. Preassembly adjustments and instrument calibrations will be made on the actuators and support system. Characteristics will be determined on the dummy system for comparison with the system installed into the stator.

The machine will be assembled with all access ports open. The purpose of the test is to insure proper assembly and alignment of sub-assemblies. Before the rotor is assembled into the machine, circumferential uniformity of axial and radial magnetic fields in the area of the rotor surface will be measured with the rotor support assembly and collector system in place. Radial and axial magnetic field will be measured at representative locations to compare with the calculated magnetic field and flux density gradients in the region of the rotor surface. With the rotor assembled, the final machining of the rotor sliprings will be checked at full field and measured at reduced field with instrumentation suitable for measuring total flux enclosed at various locations on each slipring. To determine a consistent operating point for future tests, the field will be cycled from zero to maximum and back, each time recording representative magnetic field measurements. With the brushes lifted, the rotors will be turned slowly to insure freedom. Brush actuation components will be cycled to insure proper operation. Machine internal resistance will be measured with the brushes down. The machine will be sealed, purged and filled with hydrogen. The hydrogen seals will be checked to assure integrity of the hydrogen envelope. Insulation integrity will be measured with hydrogen in the machine.

The machine rotors will be rotated at various speeds with the brushes lifted to measure windage losses with and without coolant flow and to insure proper operation of the bearings. Vibration measurements will be recorded. Comparison with subassembly tests will insure proper operation of the rotor and bearing system.

The brush actuation system will be cycled to seat and remove the brushes at various speeds. Power losses will be measured to determine brush frictional losses and to seat the brushes. This test may not be made over the entire speed range if the starting motor relies on the main machine field for operation. A reduced field and speed test may be possible; however, frictional losses may not be separable from circulating current losses in the brushes should they be significant.

The atmosphere control and cooling system will be operated to determine its proper operation. Gas samples will be withdrawn and analyzed to ascertain if the atmosphere is maintained for proper brush operation and at a level that precludes possible contamination of the hydrogen. Brushes will be cycled and the machine operated at various speeds to assure lack of contamination of the atmosphere with bearing lubricant or actuator fluid. Some adjustment may be required in internal orifices to balance the pressure drop across the rotor to eliminate thrust loads. Complete system checkout at the Westinghouse facility will not be possible since the heat loads in the machine will be only a fraction of those encountered during energy transfer pulse cycling.

As already indicated machine performance testing will be limited due to the lack of pulsed test facilities. Field current versus terminal voltage will be determined during an open circuit test. With the terminals open-circuited the machine will be operated at various levels of field excitation and speed to determine open-circuit voltage. Crossover or slipring-to-slipring circulating currents will be measured to ensure proper alignment of the rotor in the machine field. Some adjustments may be required in the field coils and/or rotor alignments to reduce losses due to crossover and brush face circulating currents to their lowest level. During open-circuit testing, brushes will be cycled to ensure satisfactory operation during the period when brush circulating currents are a maximum.

The preliminary test program will also be used to develop operating procedures for all sub-assembly systems; however, the limited test facilities may not allow complete development of operating procedures for all systems for all potential modes of operation. Insofar as possible, an operating manual for the machine will be developed.

Instrumentation for the tests may require as many as a hundred channels or sensors. Measurements will be made of both magnetic field level and direction. Temperatures will be monitored to detect localized heating and appropriate H_2 atmosphere cooling. Current distribution will be checked and voltage gradients measured. Particular attention will be given to the current collection system by observations of voltages and current. Rotor position will be determined by proximity gauges to observe misalignment, growth, and vibrations. The last item will be monitored more effectively for the machine at various stations with accelerometers. Forces and loads will be checked with strain gauges and bearing loads followed by observing the oil pressure. Flow measurements of the H_2 cooling system will be made. Rotor speeds will be observed with appropriate tachometers, possibly with a reflected light beam. Instrumentation will be installed as part of the machine fabrication.

Following the conclusion of preliminary testing, the machine will be disassembled, thoroughly examined, and reassembled.

C. LASL Facility and Tests

Tests of the 10-MJ model homopolar machine will be aimed in every respect to determine how well it meets the design criteria, namely, to deliver 10 MJ of energy with a discharge time of 30 ms and a peak current of $1.5(10)^6$ A and peak voltage of 719 V and to determine how well it satisfies variations therefrom for other applications. All the tests will be conducted in such a way to make measurements for evaluation of features of the machine which are basic to almost any homopolar.

The important characteristic features which are common to the model machine and to all homopolars of this kind are essentially those emphasized in Section IV of this proposal covering the machine design. Two types of measurements will be required, passive and active. Because of the short time periods involved in any given test, a small computer with analog-to-digital interface to the sensing elements will be needed. Passive instrumentation will be for data collection and subsequent examination whereas the active instrumentation will serve both this function and to operate the homopolar with control and safety overrides and interlocks. It is anticipated that no additional instrumentation beyond that required for the preliminary tests will be required for the homopolar.

Besides testing to evaluate the ultimate design performance of the machine, measurements of low speed and low current performance will be made first to understand the machine behavior and operation. The superconducting field coil will be operated separately and the rotor brought to full speed in several steps. The current collection system will be operated first mechanically and then electrically. Similarly, each subsystem function, i.e. bearing oil supply, gaseous H_2 cooling system, etc., will be evaluated on an independent basis prior to integrated machine operation and testing. These early system checks will also establish the instrumentation functions and reliability.

Particular emphasis in the testing will be given to brush behavior and machine stability. More specifically the tests will examine peripheral rotor speeds up to 277 m/s, the current collection system with current densities up to 1.6 kA/cm^2, brush wear, brush heating, inertial brush effects and other brush loading, H_2 atmosphere cooling, the superconducting excitation coil performance, energy transfer and efficiency, bearing loading, effects of misalignment if it exists, rotor slipring and drum growth and contraction, etc.

The facility for testing the machine will, to the extent that is practical, be made sufficiently flexible to conduct full energy transfers at reduced peak currents and longer transfer periods. A range of potential test conditions is given in Table XVII.

The final test facility configuration is subject to further detailed design study; however, preliminary analysis indicates rather clearly the direction to proceed. The test circuit is in Fig. 12. The circuit can be used in three ways. With the crowbar switch held open the start switch can be closed to discharge the homopolar machine. Energy will be transferred into the load inductor and back into the homopolar. The homopolar and the load coil comprise a resonant L-C

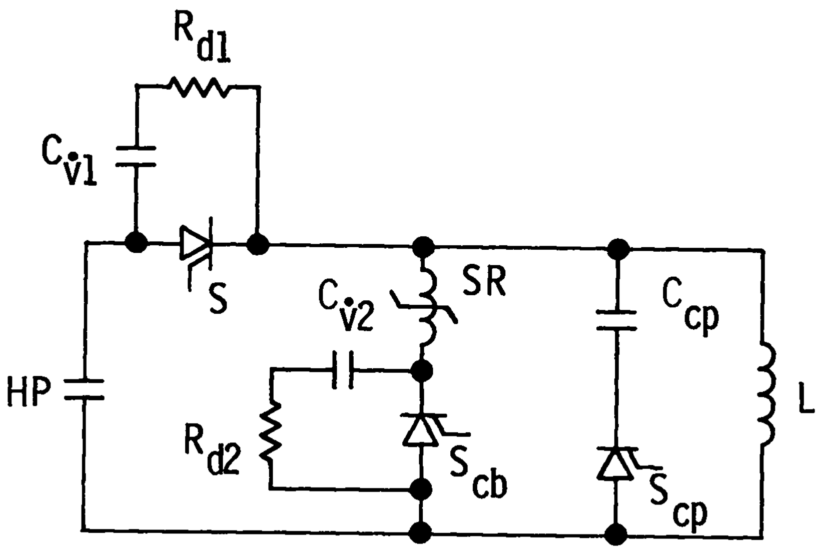

HP	Homopolar
$C_{\dot{V}1}$, $C_{\dot{V}2}$	Voltage suppression capacitors
C_{cp}	Counterpulse capacitor
R_{d1}, R_{d2}	Damping resistors
SR	Saturable reactor
S	SCR start switch
S_{cb}	SCR crowbar switch
S_{cp}	SCR counterpulse switch
L	Load inductance

Fig. 12. Homopolar Test Circuit.

TABLE XVII

TEST CONDITIONS FOR 30-ms, 10-MJ HOMOPOLAR

τ, s	I_{max}	L
1	46 kA	9.5 mH
0.5	93 kA	2.3 mH
0.3	155 kA	0.83 mH
0.03	1.55 MA	8.3 μH

circuit. The second mode of operation involves closing the start switch to discharge the homopolar followed by shorting across or crowbarring the load coil with the crowbar switch to trap the energy in the load coil. The start switch is subsequently opened at an appropriate current zero. The energy in the closed load coil loop can dissipate away with a characteristic L/R decay time in a series-connected dump resistor not shown. The third mode of operation will simulate the RTPR operating cycle with energy to be transferred back into the homopolar machine. After energy is held in the load coil, the current in the crowbar switch is brought to zero by a reverse current from the counterpulse capacitor bank. At the time corresponding to I=0 the crowbar switch is opened and energy transfers back into the homopolar. The start switch for recharging the homopolar closes shortly after the crowbar switch is opened with current flow to the counterpulse capacitor in the intervening transition period.

In devising the test facility consideration has been given to whether it should primarily serve as a systems test facility or a homopolar test facility. Good engineering practice indicates that in the absence of a designed system requiring development with the homopolar as an element of that system that the latter approach should prevail. For this reason a facility which is the most reliable is proposed with the ability to use it for further systems work as required.

These criteria have led to the comparison of vacuum interrupters and SCR's as the switching elements with a decision to use the latter. One hundred and fifty SCR's will be needed, carrying surge currents of 10 kA. Ten vacuum interrupters could easily handle the switching. An additional one hundred seventy-five solid state diodes will operate with a 100-ms L/R decay time load coil to provide the crowbar. The switches sized for the shortest transfer time, i.e., 30 ms, are safe for the longer transfer periods at the lower currents of Table XVII. The design figure of significance for the diodes is the integral of I^2 dt which cannot be exceeded. From this consideration the number of diodes connected in parallel varies inversely as the square root of the transfer period. This relation leads to the conclusion that the shortest transfer period is the most demanding. Since the dump resistor in the crowbar loop can be sized independently of the load coil to determine the decay period, the crowbar diodes are easily operated in a safe region. Operation with SCR's provides a reliable, easily controlled test circuit. Systems development with vacuum interrupters in the circuit can be readily accomplished by component replacement and using the homopolar as a proven energy storage unit.

The load coil for the test facility requires an inherent design flexibility with a long L/R time constant of several seconds to provide for a transfer period of 1 s. The configuration to be used will be a toroidal coil to eliminate stray magnetic fields. To obtain a reasonable time constant of five seconds, room temperature and cryogenic copper load coils have been analyzed. Because of the large amount of copper required, the result is heavily weighted in favor of a ℓN_2 cooled coil which takes advantage of a resistivity ratio improvement of almost ten. Such a coil will require 7.6 tons of copper. The toroid is to be made of thirty-six, ten-turn coils made of 0.64-cm by 13-cm strap. The major and minor toroidal radii are respectively 1.22 m and 0.41 m. The total radial force on the center support structure is $19(10)^6$ N or $5.3(10)^5$ N per 10° coil sector. These values are very reasonable.

The same load coil, which has a 600-ms L/R decay time at ambient temperature and 5 s at ℓN_2 temperature, can be used to meet the requirements of any of the three operational modes to be used for testing-noncrowbarred resonant energy transfer, fast energy decay after crowbarring, and RTPR-like homopolar discharge and recharge - and energy transfer over periods up to one second.

The thirty-six coils of the toroid can be series-parallel connected to provide inductances ranging from 8.3 μH to 9.5 mH corresponding to machine discharge times ranging from 30 ms to 1 s.

The ℓN_2 container for the cryogenic load coil is a conventional dewar and poses no unusual fabrication problems. It might well be made at very low cost using poured styrofoam or urethane cellular plastics for insulation.

The proposed test facility for the homopolar machine has no development problems and as such is well within existing technology. Detailed design of the facility and its operation should be straight forward. Instrumentation and controls will use conventional equipment.

VI. PROGRAM COSTS AND SCHEDULES

A. Schedule

The overall program for the development, construction, and preliminary testing of the machine at Westinghouse is planned for completion during a twenty-four-month period embracing 1977 and 1978. The program is directed at sequential events and concurrent events which lead to the delivery of the demonstration machine to Los Alamos at the end of the two-year period. The schedule is presented in Fig. 13.

The proposed program schedule is presented below:

Task 1 - The brush loading device will be developed and extensive tests conducted on a test rig at speeds ranging up to 277 m/s. A number of devices will then be tested together on the same slipring. Several brush grades will be evaluated in the loading device.

Task 2 - The aluminum rotor fabrication processes will be developed and a rotor constructed. After testing and evaluation the rotor will be sectioned for metallurgical examination. Process specifications for the machine rotors will be developed.

Task 3 - The center superconducting magnet will be built and tested in a helium dewar. All of the important parameters and characteristics will be determined.

Task 4 - Manufacturing Drawings. The drawings required to construct the machine will be developed from the detailed design and also from the results of tasks 1, 2, 3, and 5. These drawings will completely specify the dimensions, materials, and process requirements for each of the components and the overall machine.

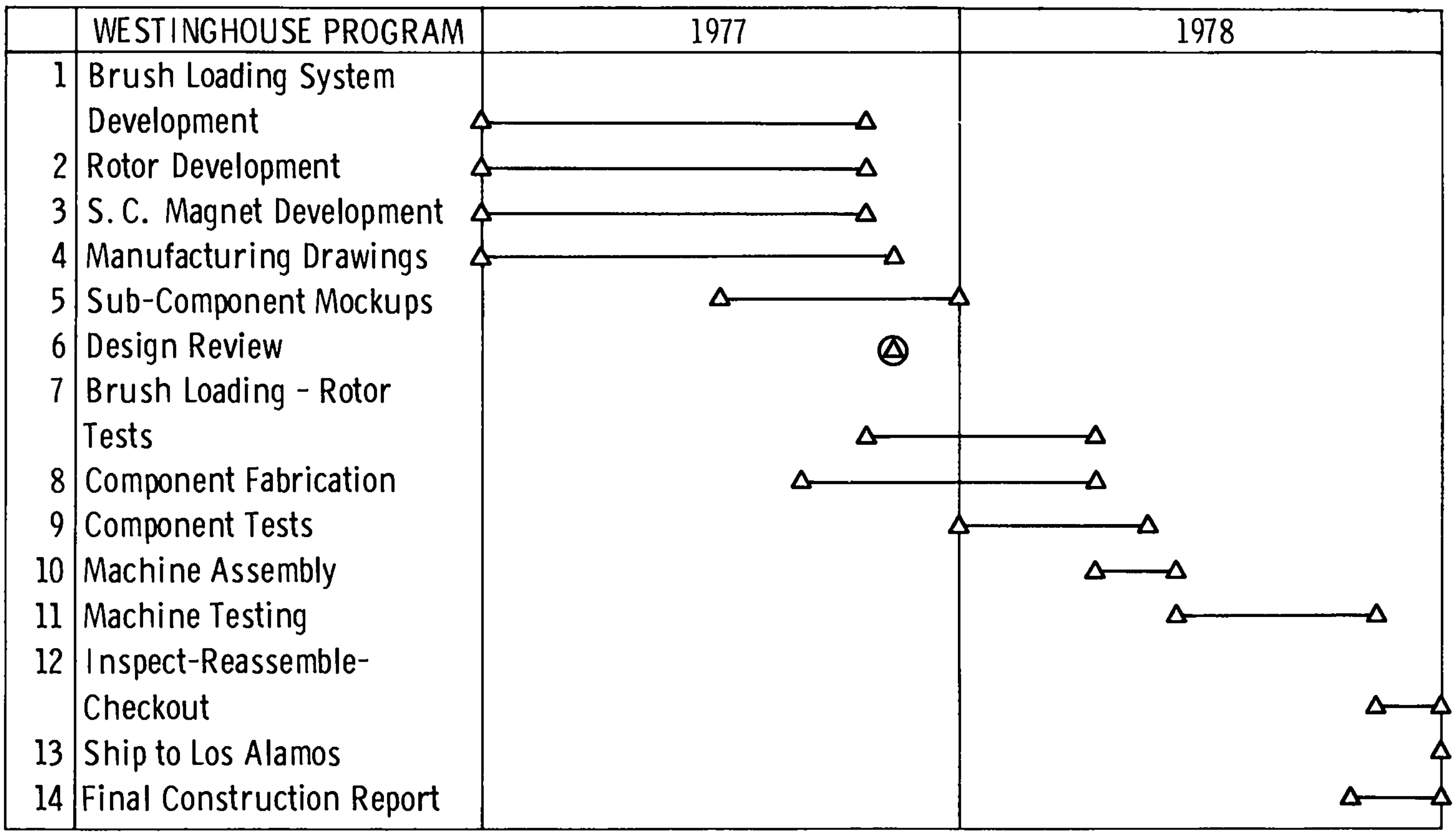

Fig. 13. 10-MJ, 30-ms Model Homopolar Machine Construction and Test Schedule.

Task 5 - Subcomponent Mockups. These fabrications are required to verify or determine processes used for the machine component fabrication.

Task 6 - Design Review. A complete review of the design is proposed.

Task 7 - Brush Loading - Rotor Tests. Large groups of brushes will be tested simultaneously in a test rotor using simulated machine sliprings and actual machine bearings. These tests will provide for evaluation of brush group actuation and operation at various speeds under conditions similar to those in the model machine.

Task 8 - Component Fabrication. Components will be fabricated in accordance with the drawing requirements.

Task 9 - Component Testing. All components will be inspected and tested to ensure compliance with the design and drawings.

Task 10 - Machine Assembly. The machine will be assembled keeping meticulous records of dimensions, fits, and electrical measurements.

Task 11 - Machine Tests. Extensive tests will be conducted in accordance with the test program.

Task 12 - Inspect - Reassemble - Checkout. Subsequent to the test program the machine will be dismantled and inspected for wear, defects, and problem areas. The machine will be cleaned, adjusted, reassembled,and checked out completely.

Task 13 - Ship to Los Alamos. The machine will be packaged for shipment.

Task 14 - A report on the complete twenty-four-month program will be assembled.

The schedule for building the test facility and performing tests at LASL starts with facility design to be completed in FY77, ordering and receipt of components in FY's 77 and 78, facility construction in FY78, facility checkout in FY's 78 and 79, homopolar testing in FY79, and report drafting in early FY80. This schedule is shown in Fig. 14.

B. Cost

The overall machine costs for the model machine include design, development, construction, testing, and construction of a pulsed test facility at LASL. Significant costs are associated with the process development and management of the fabrication and testing program.

The first year's cost results mainly from the design and development activities with some fabrication and component testing and component purchase for the pulsed test facility. The second year's efforts are for machine fabrication and

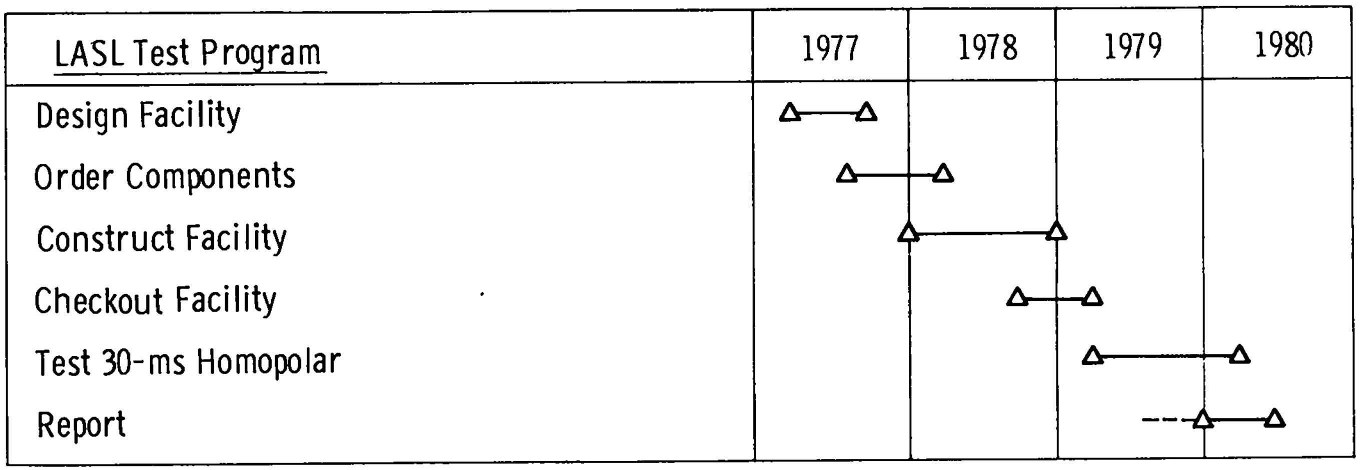

Fig. 14. LASL Homopolar Facility and Machine Test Schedule.

testing, pulsed test facility component purchase, and construction and checkout of the pulsed test facility. The third year's cost is for testing the model homopolar with a small fourth year cost for report drafting on the machine test results. The first year's cost has four major components, namely, engineering and drafting, current collection development, superconducting magnet development, and aluminum rotor development by Westinghouse and test facility development by LASL.

The first year's costs are presented in Table XVIII for Westinghouse and in Table XIX for LASL.

TABLE XVIII

FY-77 HOMOPOLAR MACHINE COSTS (WESTINGHOUSE)

Engineers and Scientists	HRS	
Project and Mechanical	3600	
Superconducting Magnet Technology	950	
Brush Loading	1300	
Brush Technology	640	
Electrical	700	
Process Development	640	
Total	7830	$282,300
Drafting	2000	
Computer		$ 4,600
Subtotal		$286,900
Current Collection and Brush Technology (Materials and Technicians)		
Basic Loader Development		$ 82,100
Brush-rotor Test System		$ 78,330
Subtotal		$160,430
Superconducting Magnet Development and Testing		
Center Magnet Construction		$215,786
Magnet Testing		$ 27,000
Subtotal		$242,786
Aluminum Rotor Development		$ 49,400
Data Acquisition and Sensing System		$ 48,800
Subtotal		$ 98,200
Total		$788,316

TABLE XIX

FY-77 HOMOPOLAR MACHINE COSTS (LASL)
TOTAL PROGRAM*

		President's Budget
Personnel - Direct Expenses	$ 63,000	$ 63,000
Indirect Expenses	34,000	34,000
Materials, Services, and Subcontracts	17,000	17,000
Major Procurement		
10-MJ Homopolar	788,316	650,000
Voltage ~~com~~suppression capacitors	(on hand)	(on hand)
Start switch	45,000	45,000
Counterpulse switch	30,000	30,000
Busbar	22,684	11,000
Subtotal (Major Procurement)	$ 886,000	$ 736,000
Total	$1,000,000	$ 850,000

*EPRI portion of cost included.

Capital equipment FY77 $65,000

The total FY77 cost is $1,000,000 operating expense and $65,000 capital equipment expense. Of the operating expense, it is proposed that $400,000 is to be the EPRI portion of the cost. The president's budget level will slow homopolar development by about three months.

The FY78 costs consist of construction and testing costs with the support of the engineering effort required to direct the program and costs associated with completion of purchase of the pulsed test facility components, their installation, and checkout. These are presented in Tables XX and XXI.

The total FY78 cost is $1,751,832 operating expenses and $50,000 capital equipment expense. Of the operating expense, it is proposed that $200,000 is to be the EPRI portion of the cost. The FY79 and FY80 costs are respectively $260K and $120K for testing and reporting by LASL.

VII. FUTURE PROGRAMS

A. Use of the 10-MJ Machine

The primary application of the 30-ms, 10-MJ fast discharge homopolar has been set forth in Sections I, II, and III of this proposal as a model of larger machines for driving the SFTR and the RTPR. Of immediate interest and application, once the model machine has been thoroughly tested, is the use of the 10-MJ homopolar as a pulsed energy source for a linear theta-pinch experiment, toroidal pinch devices, fast liner experiments, and for tokamak ohmic-heating development[29] discussed briefly below.

1. Linear Theta Pinch With Improved End Stoppering and/or Marshall Gun Injection: The presently preferred end-stoppering methods are high-density gas and/or solid end plugs and moving multiple mirrors. The use of Marshall gun injection is a possible alternative to shock heating of the plasma. Both shock heating and

TABLE XX

FY78 HOMOPOLAR MACHINE COSTS (WESTINGHOUSE)

Engineers and Scientists		HRS	
Project and Mechanical		3200	
Superconducting Magnet Technology		800	
Brush Loading		1000	
Brush Technology		400	
Electrical		600	
Process Development		200	
Total		6200	$230,327
Drafting		640	
Computer			$5,000
Subtotal			$235,327
Construction Cost	**Shop & Technician-HRS**		**Materials**
2 End Magnets	4560		$139,838
2 Rotors	1300		11,523
2 Bearings	800		4,880
Magnet Suspension	500		4,900
Brush Loading System	2770		8,500
Cross-over Assembly	700		2,195
Drive Motors	877		1,280
Iron Shell	2400		27,450
Stator Winding	600		5,260
End Closures	600		4,890
Sensors - 250	330		14,300
Piping and Ducting	260		3,170
Machine Assembly	2240		
Machine Testing	3800		
Machine Inspection & Reassembly	2200		12,000
Auxiliaries			$ 46,960
Hydrogen Blower			
Heat Exchanger			
Evaporator			
Oil Lube System			
Actuator Hydraulics			
Hydrogen Control			
Subtotals			$287,146
	23937		$461,859
Total			$984,332

TABLE XXI
FY78 HOMOPOLAR MACHINE COSTS (LASL)
TOTAL PROGRAM*

Personnel - Direct Expenses	$ 154,000
Indirect Expenses	83,000
Materials, Services, and Subcontracts	65,000
Major Procurement	
10-MJ Homopolar	984,332
Counterpulse capacitor	90,000
Damping resistors	1,000
Saturable reactor	2,000
Crowbar switch	55,000
Load Inductance	300,000
Dewar	17,500
Subtotal (Major Procurement)	$1,449,832
Total	$1,751,832

*EPRI portion of cost included. Capital equipment FY78 $50,000

gun injection require low-energy, high-voltage capacitor systems for staging into a slow-compression long solenoid. This solenoid has a field risetime of from 1 to 20 ms depending on whether the system is pure fusion or fission-fusion. Such slow-rising compression fields will be furnished by magnetic energy storage and breaker-type switching. The energy could be obtained from either the superconducting METS or a pulse-sharpened homopolar system consisting of the following components: HETS-type fast discharge homopolar which energizes aluminum storage coils whose current is broken by an interrupter and transferred into the slow compression theta pinch. An alternative to magnetic energy storage for linear theta pinches is direct excitation by means of a fast-drive homopolar in the 1-20 ms range.

2. Toroidal Pinch Devices: The reversed field pinch is being developed through the sequence ZT-1, ZT-S, ZT-P. This high-beta experimental program is expected to go to the ZT-2 feasibility experiment and possibly on to reactor systems. The ZT-2 experiment will require a 20-50 ms power crowbar pulse which is an additional application for the fast HETS homopolar.

The sustaining field current required for the ZT-P may be as high as 600 kA with a driving potential of several hundred volts for a period up to several milliseconds. For the ZT-2 the sustaining current could be as high as 5 MA for a period of tens of milliseconds. The impedance of these machines is low, being 17 μ-ohm and 1.7 μ-ohm, respectively. The connecting bus bar impedance dominates the circuit and impedance matching to a homopolar can be accomplished.

LASL is proposing a high-beta tokamak program to test toroidal confinement in the β = 20% range. Like other pulsed high-beta devices it is staged, beginning with low-energy capacitor drive, fast crowbarred, and then power crowbarred for long confinement by a fast HETS in the 10-100 ms range. The feasibility experiment could be constructed this way, depending on the ability of tokamaks to support such high beta.

3. Fast Liner Experiment: A very high-density fusion concept is the fast liner compression device utilizing magnetic fields of approximately 5-10 MG, burn times of 1-10 μs, and density of 10^{19} - 10^{20}cm^{-3}. A similar program is under way at NRL which uses slow compression at about 2 MG with burn times of 100 μs. The proposed LASL approach, which is quite similar to that at Krasnya Pachra and Leningrad in the USSR, will utilize magnetic energy storage to drive the liners with risetimes of about 100 μs and dwell times (= burn times) of 10 μs. Such energy storage will most likely be aluminum or copper coils excited by fast homopolar with discharge times from 20 to 200 ms and with current interruption either by means of vacuum breakers or some other form of air or gas breaker.

4. Tokamak Ohmic Heating: An ERDA sponsored study to evaluate tokamak ohmic-heating systems is under way with LASL, University of Texas, and Westinghouse participation. The anticipated pulsed energy source for tokamak ohmic-heating is a slow discharge (0.25-1.0 s) homopolar. This requires heavy rotor, higher voltage homopolars than the pulsed high-density work, but it shares in an essential way the common elements of high peripheral speed rotors, high-current density brush collection systems, and superconducting field coils.

It is clear that magnetic energy storage and switching and fast discharge homopolars are not limited to the SFTR, RTPR toroidal theta-pinch systems. Fast discharge homopolar machines of the HETS type can be used for direct drive of long pulsed linear theta pinches, toroidal Z pinch, and high-beta tokamak devices. Modified, somewhat slower homopolar machines can be used to power tokamak ohmic-heating field coils. In addition they are ideal, cheap energy storage sources for exciting aluminum or copper energy storage coils to drive shorter pulsed linear theta pinches (appropriate to fusion-fission or near-term fusion feasibility experiments) as well as liner fusion test reactors and demonstration plants.

B. Conversion to Slower Discharge Times

The 30-ms, 10-MJ fast discharge machine can be operated over a longer discharge period at reduced currents merely by increasing the inductive load as indicated in Section V above. This will provide important test data bearing on machine performance and its subsystems. To conduct an ultimate experiment on a slower discharge homopolar will require retrofitting with a heavier rotor into the stator of the 30-ms, 10-MJ machine. If the presently planned model machine is retrofitted with a segmented iron rotor with the segments connected in series, then, with somewhat reduced speeds, a 30-50 MJ capacity homopolar can be built. The series-connected segmented rotor will provide an output voltage of about 2.5 kV. The use of a heavy rotor will undoubtedly require a redesign of the bearing system. The higher voltage heavy rotor, slower discharge machine will operate in the 250-ms to 1-s range with currents of several hundreds of kilo-amperes. Such a machine will closely model the pulsed energy source requirements for a tokamak ohmic-heating system.

VIII. ADMINISTRATIVE ARRANGEMENT

A. Cooperative ERDA-EPRI Funding

This proposal is for the completion of the manufacturing design, component development, construction, and testing of a 10-MJ, 30-ms discharge period model homopolar machine. It is proposed that the program be conducted with joint funding by ERDA and EPRI and that the EPRI share be $400,000 for 1977 and $200,000 for 1978. It is further proposed that the balance of the funding be by ERDA.

B. Technical Direction

The work of this proposal is to be done under the supervision of the Los Alamos Scientific Laboratory with Fred L. Ribe and Keith I. Thomassen as the principal investigators for the program. Manufacturing design, component development, and construction and preliminary testing of the homopolar are to be a Westinghouse responsibility under the direction of C. John Mole. Program accountability at Westinghouse will be to Zalman M. Shapiro, Manager, Fusion Power Systems Department. Work at Westinghouse is to be performed by personnel of the Research and Development Center and the Electro-Mechanical Division. Additional technical oversight of the work at Westinghouse and the pulsed testing of the homopolar will be performed by personnel of group CTR-9 at LASL under the direction of John D. Rogers. Of particular interest in this respect is the recent addition to the LASL staff of personnel, Philip Thullen and James Weldon, with experience in the fields of superconducting rotating machinery, homopolars, and high current collection or brush systems.

C. Contractural Arrangements

For the homopolar program it is proposed that funding from both ERDA and EPRI be direct to LASL and that a single contractural agreement between Westinghouse and LASL be established for the work to be performed by the former. An appropriate contract between EPRI and LASL should be formulated to provide for this arrangement and for further LASL responsibilities to EPRI. ERDA funding presumably will be provided through already established channels. A single contract for performance of the design, component development, construction, and preliminary testing will create a direct line of supervision and responsibility.

Reporting is to be monthly by brief letter reports from Westinghouse to LASL. Information included in the monthly reports will cover (1) technical progress, (2) maintenance of work to the schedule, and (3) costs accumulated. LASL will report monthly on technical progress and forward the report, incorporating the Westinghouse report, to ERDA and EPRI. LASL will also report on the program in their regular quarterly progress report. A semiannual program review is to be held with Westinghouse and LASL personnel reporting to ERDA and EPRI on progress, plans, schedule, and costs. A semiannual report covering the review is to be submitted by LASL. A technical review of the finished homopolar machine design is to be held as provided in the schedule of Task 6 of Fig. 13. Final technical reports on the work will be written by Westinghouse and LASL.

Contract monitoring is intended to be accomplished by following progress on tasks and costs associated therewith. Technical progress for each task will be evaluated to formulate program redirection as needed.

REFERENCES

1. K. I. Thomassen et al., "Conceptual Design Study of a Scyllac Fusion Test Reactor," Los Alamos Scientific Laboratory Report LA-6024; Los Alamos, NM, January 1976.

2. J. D. Rogers et al., "Proposed METS-FTR Coupled Superconducting Prototype System," Los Alamos Scientific Laboratory Report LA-5918-P; Los Alamos, NM, April 1975.

3. F. L. Ribe, R. A. Krakowski, K. I. Thomassen, T. A. Coultas, "Engineering Design Study of a Reference Theta-Pinch Reactor (RTPR)," Special Supplement on "Fusion Reactor Design Problems" to Nuclear Fusion; International Atomic Energy Agency, Vienna, 1974.

4. P. J. Turchi, A. E. Robson, "Conceptual Design of Imploding Liner Fusion Program," Proc. Sixth Symp. Eng. Problems Fusion Research; San Diego, Nov. 18-21, 1975.

5. R. E. Stillwagon, "Design Studies of Reversible Energy Storage and Transfer Systems for the Reference Theta-Pinch Reactor," Westinghouse Report E. M. 4620; Pittsburg, PA, September 1974.

6. R. E. Stillwagon, "Optimization Study of Homopolar Energy Transfer System for the Reference Theta-Pinch Reactor," Westinghouse Report E. M. 4736; Pittsburgh, PA, August 1975.

7. K. I. Thomassen, "Conceptual Engineering Design of a One-GJ Fast Discharge Homopolar Machine for the Reference Theta-Pinch Fusion Reactor," Semiannual Report to EPRI, July 1975, to be published.

8. R. A. Krakowski et al., "Prospects for Converting ^{232}Th to ^{233}U in a Linear Theta-Pinch Hybrid Reactor (LTPHR)," DCTR Fusion-Fission Energy Systems Review Meeting, ERDA-4; Germantown, MD, Dec. 3-4, 1974.

9. H. F. Vogel,et al., "Energy Storage and Transfer with a Homopolar Machine for a Linear Theta-Pinch Hybrid Reactor," Los Alamos Scientific Laboratory Report LA-6174, Los Alamos, NM, April 1976.

10. R. A. Feranchak, "Economic Optimization Study of Energy Storage and Transfer Systems for Los Alamos Scyllac Fusion Test Reactor," Westinghouse Electric Corp. Report E. M. 4746; Pittsburgh, PA, Aug. 1975.

11. K. I. Thomassen, "Reversible Magnetic Energy Transfer and Storage Systems," Proceedings of Texas Symposium on CTR Technology and the Engineering Aspects of Fusion Reactors, Austin, Texas, November 1972.

12. M. D. Driga et al, "Fundamental Limitations and Topological Considerations for Fast Discharge Homopolar Machines," to appear in IEEE Trans. on Plasma Science.

13. E. Gregory, W. G. Marancik, and F. T. Ormand, IEEE Trans, Mag., MAG-11, 295 (1975).

14. P. Blum, D. L. Coffen, and E. Gregory, "Some Investigations on a Ductile Multifilamentary Nb_3Sn Conductor and the Performance of a Magnet Made From It," Presented at 1975 Cry. Eng. Conf., Kingston, Ontario.

15. "Carbon Brushes for Industrial Machines," Brochure produced by LeCarbone (Gt. Britain) Ltd.

16. "Brush Grades and Characteristics," Brochure produced by Morganite Carbon, Ltd. (UK).

17. I. R. McNab and G. A. Wilkin, "Carbon Fibre Brushes for Superconducting Machines," IEEE Journal "Electronics and Power," January, 1972, page 8.

18. I. R. McNab and G. A. Wilkin, "Life Tests with Carbon Fibre Brushes," Sixth International Conference on Electric Contact Phenomena, 1972.

19. J. L. Johnson, private communication.

20. A. Stebbens and H. Ward, "The Design of Brushes for the Homopolar Generator at A. N. U.," ANU Report EP-RR-18, March 1964.

21. D. J. Ortloff, "The Design of a Brush Test Machine and the Verification of the Machine Design and Brush Design Under Test Conditions of High Current Densities and High Relative Surface Velocities," M. Sc. Thesis, University of Texas, Austin, January 1975.

22. W. F. Weldon, private communication.

23. J. L. Johnson, discussion following ref. 26.

24. J. L. Johnson and L. E. Moberly, "Copperdrag - its Cause and Cure," Westinghouse Research Report 74-7B6-SLIDE-R1, Pittsburgh, PA, September 1974.

25. R. A. Marshall, "The Design of Brushes for the Canberra Homopolar Generator," ANU Report EP-RR-3, January 1964.

26. R. A. Marshall, "Design of Brush Gear for High Current Pulses and High Rubbing Velocities," IEEE-PAS-85(11), 1117, November 1966.

27. R. A. Marshall, "Tests with Solid Brushes on the Canberra Homopolar Generator," Nature, December 12, 1964, p. 1079.

28. L. E. Moberly, private communication.

29. F. L. Ribe, "The Role of Energy Storage in the LASL Pulsed High-Density Program," Los Alamos Scientific Laboratory internal report, Los Alamos, NM, April 1976.

☆U.S. GOVERNMENT PRINTING OFFICE: 1976-677-343/168